MOLECULAR SIMULATION
2020, VOL. 46, NO. 14, 1094–1115
https://doi.org/10.1080/08927022.2020.1804564

Mathematical and computational models of RNA nanoclusters and their applications in data-driven environments

Shyam Badu[a], Roderick Melnik [a,b] and Sundeep Singh [a]

[a]MS2Discovery Interdisciplinary Research Institute, Wilfrid Laurier University, Waterloo, Ontario, Canada; [b]BCAM-Basque Center for Applied Mathematics, Bilbao, Spain

ABSTRACT

Ribonucleic acid (RNA) is a fundamental molecule having several favourable structural properties that can be used for various potential applications in the field of nanotechnology including biomedicine and bioengineering. Here in this review, we describe the computational and mathematical modellings of the RNA nanoclusters, such as the molecular dynamics simulation, coarse-grained modelling and continuum modelling. The RNA nanocubes, nanotubes and nanorings are some of the typical nanosized structures derived from RNA strands, and the details about such nanostructures have also been presented in this review. The RNA nanoprisms made out of the RNA building blocks via self-assembly of the RNA nanotriangles and their potential applications have been described. Furthermore, special attention is given to the earlier developed RNA nanoscaffolds from the RNA building blocks. We also present some recent results to describe the physical behaviour of the RNA nanotubes in different kinds of physiological solutions using molecular dynamics simulations. Finally, the recent applications of these computational models in several areas of medical sciences such as radiotherapy and drug delivery for cancer treatment and construction of RNA nanodevices have been highlighted. Several potential applications of artificial intelligence in this fast-growing field of RNA engineering have also been presented.

ARTICLE HISTORY
Received 28 May 2020
Accepted 18 July 2020

KEYWORDS
RNA nanoparticles; nanotubes; bionanotechnology; computational modelling; artificial intelligence based methods

1. Introduction

The field of RNA nanotechnology has received tremendous attention and progressed rapidly in the past decade owing to its huge potential in the treatment of various diseases [1–6]. Following DNA nanotechnology, RNA nanotechnology has rapidly evolved aiming at building architectures from programmed self-assembly of RNA nanostructures that can be exploited in a variety of applications ranging from physical devices to nanomedicines [7]. The advancement in the field of RNA nanotechnology can be significantly attributed to the pre-existing research and knowledge in the field of RNA biology, as many of the RNA nanoparticles: (a) use previously discovered functional RNAs (viz., ribozymes, riboswitches and micro RNA (miRNA)) by the traditional RNA biology, and (b) take advantage of RNA motifs discovered by the RNA structural biologists [5,8–13]. RNA biomacromolecules can be viewed as sophisticated architectures built from simple building blocks via modular assembly and connected via different linker sequences. Many types of secondary and tertiary structures of RNA motifs have been discovered and characterised in the past decade. Accordingly, varieties of RNA architectures can be engineered by exploiting this diversity and structural flexibility of RNA motifs by utilising precise control of their shape, size and stoichiometry. Different types of RNA exist in nature that are involved in performing many vital functions. For example, the messenger RNA is involved in copying and carrying the genetic information, transfer and ribosomal RNAs represent essential translational machinery, and the gene expression is regulated by the miRNA, small interfering RNA (siRNA), aptamers, riboswitches, ribozymes and other types of RNA [5,14]. Among these, siRNA is one of the most popular types of RNA that enters the cell via interaction with cytoplasmic proteins of the cell. The recent developments in the applications and procedures of siRNA in the field of nanomedicine have been presented in a comprehensive review of Resnier et al. [15].

RNA nanotechnology involves the multitude of RNA motifs (e.g. bulges, hairpin, stems, loops and junctions) that acts as a building block for the construction and design of RNA nanoparticles [5,16]. Their physiochemical properties can be easily fine-tuned for fabricating the desired nanoparticles for a variety of in vitro and in vivo applications, such as making of the scaffold, targeting ligands, therapeutics agents, regulatory modules and imaging agents, etc. [5,14]. The specific assembly of the RNA nanoscaffold has been presented in [17] utilising the coarse-grained method based elastic network modelling. The RNA motifs are attached with an emerging class of target ligands known as RNA aptamers that similar to protein antibodies assist in binding with high affinity and specificity to their target. The integration of aptamers to RNA nanoparticles can guide them to their target receptor molecule overexpressing regions and facilitating cell entry via receptor-mediated endocytosis [3]. The typical binding of the RNA aptamer with the GTP has been shown in Figure 1, as described in the PDB entry 5LWJ [18]. Several studies have been reported in the literature on the clinical trial of the RNA aptamers, their

CONTACT Sundeep Singh ssingh@wlu.ca

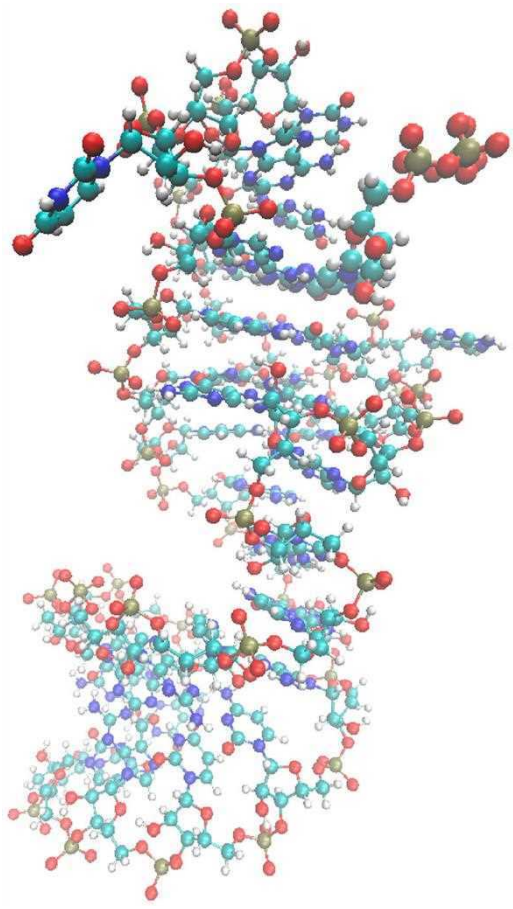

Figure 1. (Colour online) VMD generated structure of the RNA interaction with the ligand taken from the PDB code 5LWJ.

modelling and applications in the field of cancer treatment [19–23]. The affinity of the RNA aptamers generally depends on the sequence of the nucleotides present in the aptamer. Several numbers of RNA sequences are possible for a particular RNA aptamer with the same number of nucleotides or for a specific target molecule such as a ligand, a specific sequence of the RNA aptamers will be the best fit. A computational technique has been proposed to generate several numbers of potentially favourable sequences of the aptamers for binding to the host along with the criteria for their selection that will eventually facilitate the experimentalists to choose a set of suitable aptamers for the desired applications [22,24]. Moreover, the DNA aptamer's interaction with the small macromolecule or the ligands can also be used for the variety of different applications in biomedicine. A detailed study of the DNA aptamer binding with particular kinds of the ligands utilising computational docking methods has been presented in [25].

The theoretical and computational techniques have been extensively utilised for studying and predicting the RNA structure and their interactions with the ions and ligands, for e.g. in [26–28]. Computer modelling methods have also been used for designing and optimisation of the derived nanostructure [29–32]. More recently, a new approach has been presented in [33] for mitigating the need for human intuition in designing the three-dimensional structural design of RNA by reducing the problem to pathfinding problem that can be automatically solved using novel RNA algorithms. Studies are also available in literature regarding the combination of the siRNA with the super paramagnetic iron oxide nanoparticles and the linear polysaccharide compounds to form a magnetic nanovector that can be used for cancer treatment [34,35]. Furthermore, experimental techniques have also been developed to improve the applicability of the magnetic siRNA nanovectors via calculation of the surface plots and hydrodynamics diameters [35]. The effectiveness of delivery of siRNA based on the properties of nanoparticles, viz., particle size, loading capacity and encapsulation capacity have been described in [36,37]. Importantly, these studies revealed that the optimisation of nanoparticles is quite essential for enhancing their performances. The nanoparticles formed from the metal-organic compound, such as chitosan polymer has been tested for targeted delivery on mice and it was found that this technique was far more effective as compared to the non-targeted delivery [38–40]. Several structures of the nucleic acid self-assemblies of the different shapes and sizes such as the dimer, trimmer, tetramers, etc. have also been modelled using different techniques, as reported in previous studies available in literature [41–49]. Like RNA nanoclusters and self-assemblies, there are several applications of the DNA self-assemblies as well as their complexes with other nanosystems. The gold nanoparticles modified by the interaction with the DNA have also been tested for its delivery capacity for the oligonucleotides of RNA in [50]. In another work the interaction of the RNA with small molecule ligands has been reviewed on the basis of their computational modelling [51]. Several other studies have been reported in the literature addressing the structure and binding characteristics of the DNA aptamers with the ligand and other metal structures [52–54]. Also the potential application of the RNA nanoclusters and their computational modelling has been extensively discussed in [55–57]. Among other models, this review includes the computational models of the RNA self-assembled nanostructures that can be used for the cancer therapy and treatment of other diseases in human body. Furthermore, the reaction mechanism and the related energetics in the hydrolysis reaction occurring at the editing domain of the *Thermus thermophilus* leucyl-tRNA (LeuRS) system has been inspected in [58], utilising the hybrid quantum mechanics/molecular mechanics (QM/MM) approach.

The rest of this paper is organised as follows. In Sections 2, the mathematical background of different computational techniques used for modelling and studying properties of RNA nanostructures from their building blocks have been provided. The application of the computational modelling in development of RNA nanoclusters, viz., nanoscaffolds, nanoprisms and other topological configurations have been provided in Sections 3. The results of recent studies on the molecular dynamics simulation, coarse-grain modelling and atomistic-to-continuum based simulation of RNA nanotubes in the physiological solutions have been presented in Section 4. In Section 5, potential applications of the RNA nanoclusters are discussed in the context of disease treatments, drug delivery and nanodevices fabrication in medical imaging, along with most recent application of the artificial intelligence in field of RNA engineering. Concluding remarks and outlook have been provided in Section 6.

2. Current methodological approaches

In this section, we will describe some of the key theoretical and mathematical techniques used for modelling of the RNA nanoclusters, their self-assemblies and their interaction with other biomolecules involved in the biological processes such as cell membranes, ligands, etc.

2.1. Molecular dynamics simulation

The molecular dynamics simulation is one of the most important techniques used to study the properties, interaction, modelling and optimisation of the various molecular systems, most commonly the biomolecules including the nucleic acid systems [59–62]. Due to the rapid increase and wide availability of computational resources, the application of classical molecular dynamics simulation for describing the behaviour of complex biomolecular systems has become quite popular in the past few decades [59,62–66]. Importantly, in the molecular dynamics simulation, the classical equations of motion of a molecular system are solved by their time-dependent integration. The potential of the system used during the molecular dynamics simulation using the chosen force field can be expressed as follows:

$$\begin{aligned} V_{total} = & \sum_{bond} K_b(r - r_0)^2 + \sum_{angle} K_\theta(\theta - \theta_0)^2 \\ & + \sum_{dihedral} K_\phi(1 + cos(n\phi - \gamma)) \\ & + \sum_{Hbond} \left(\frac{C_{ij}}{r_{ij}^{12}} - \frac{D_{ij}}{r_{ij}^{10}}\right) + \sum_{van\ der\ Waals} \left(\frac{A_{ij}}{r_{ij}^{12}} - \frac{B_{ij}}{r_{ij}^{10}}\right) \\ & + \sum_{Coulombic} \frac{q_i q_j}{\epsilon r_{ij}}, \end{aligned} \tag{1}$$

where the first term corresponds to the bonds that counts each covalent bond in the system, the second term corresponds to the angles, i.e. the angles between each pair of covalent bonds sharing a single atom at the vertex, the third term corresponds to the dihedral that describes the atom pairs separated by exactly three covalent bonds with the central bond subjected to the torsion angle (ϕ), the fourth term defines the interaction coming from the hydrogen bonds which includes the base pairing as well as the hydrogen bonding between the RNA and the water molecules, the fifth term represents the long distance interactions known as the (van der Waals' interactions) and the last term represents the electrostatic interaction term of the Coulomb form (where q_i and q_j represents the partial atomic charges of atoms i and j separated by a distance r_{ij}). The parameters K_b, K_θ and K_ϕ are the bond stretching, bond bending and dihedral angle torsional force constants, respectively, r is the bond length, θ is the bond angle, ϕ is the dihedral angle, the variables with the subscript '0' are the respective equilibrium values, n is the multiplicity or periodicity of the dihedral angle, γ is the phase shift and ε is the effective dielectric constant.

From the above expression for the total potential energy of the system, it is quite clear that the energy is a function of the positions of particles. If the position (x) of the particle at a time t is known, then its value after the time step δt i.e $t + \delta t$ can be calculated by Verlet (Equation (2)) and the velocity-Verlet (Equation (3)) algorithms derived from the Taylor expansions that can be easily coded in any molecular dynamics simulation software (e.g. NAMD and AMBER), and was originally proposed in [67] as follows:

$$x(t) = x_0 + v_0 t + a_0 \frac{t^2}{2} + \cdots\cdots, \tag{2}$$

$$x(t + \delta t) = x(t) + v(t)\delta t + \frac{F(t)}{m}\frac{\delta t^2}{2} + \cdots\cdots, \tag{3}$$

where x is the position, t is the time, v is the velocity, F is the force and m is the mass of particle.

The velocity of an atom at time t and $t + \delta t$ can also be calculated by using the acceleration of the atom, similar to the way the position is calculated from the velocity based on Equations (2) and (3). From the potential energy of the system the acceleration of the k^{th} particle can be calculated from Newton's equation of motion as:

$$a_k(t) = -\frac{1}{m}\frac{dv_{total}}{dr_k(t)}. \tag{4}$$

Alternatively, the force of an atom during the molecular dynamics simulation can be expressed as:

$$F_k(t) = m_k \frac{d^2 r_k(t)}{dt^2} = \frac{dv}{dr}, \tag{5}$$

where the $r_k(t)$ is characterised by the coordinates $(x_k(t), y_k(t), z_k(t))$ in the three-dimensional space.

The total potential energy of the system in absence of the external force can be expressed as:

$$U = \sum_{i=1}^{N}\sum_{i>j}^{N} u(r_{ij}). \tag{6}$$

One of the most common potential describing the large distance interactions, e.g. van der Waal's interaction, is the Lennard-Jones potential which can be expressed as [68]:

$$u_{LJ}(r_{ij}) = 4\epsilon\left[\left(\frac{\sigma}{r_{ij}}\right)^{12} - \left(\frac{\sigma}{r_{ij}}\right)^{6}\right], \tag{7}$$

where the parameter ε governs the strength of the interaction and σ defines a length scale. Basically, this interaction repels at close range, then attracts, and eventually cut-off at some limiting separation.

During the molecular dynamics simulations, consideration of this kind of potential is extremely important for studying the long range interactions, such as the binding of the ligand with the RNA nanoclusters and RNA aptamers. Furthermore, comprehensive details about the application of molecular dynamics simulations in the modelling of RNA molecules can be found in [69–71].

2.2. Coarse-grained modelling

There has been a considerable development in the area of computational techniques for modelling nanoscale biological

structures, owing to the availability of huge computational resources for including simulation samples as large as possible [72–75]. However, certain features of biological processes still cannot be addressed thoroughly due to a large time scale of their occurrence. Therefore, the coarse-grained models are designed to explain information about the system at such larger scales from the smaller scale that are modelled starting from the atomistic classical approach. A comprehensive overview of the coarse-grained models for accessing long time scales in simulations of biomolecular processes focusing on the modelling of proteins structure, dynamics and interactions have been reported in [76–78]. Importantly, during the coarse-grained modelling the groups of atoms are represented by coarse-grained interaction centres (known as beads) and the effective interactions between such beads is fitted utilising the nanostructure's atomic connectivity, thermal, mechanical and other properties. There are two commonly used approaches in this fitting process: (a) the experimentally available structural information, and (b) very detailed atomistic data obtained from all-atom molecular dynamic simulations [79,80]. Notably, the parameters for a coarse-grained model can be derived from both experimental and full-atom molecular dynamics data by Boltzmann inversion [81] of the radial distribution functions using the inverse Monte Carlo scheme (also known as Newton inversion method) [82] or, with the 'force matching' method in the case of all-atom molecular dynamics simulation [83].

The developed coarse-grained models should be easy enough to accurately simulate the physical characteristics of the system. Firstly, in the coarse-grained modelling, the sum of atoms as a pseudo atom is represented and then an effective energy function is defined (U_{CG}) for determining the thermodynamical properties, which should be identical to the system's properties once the proper energy function is predicted. Studies have been reported in previous literature utilising the coarse-grained modelling approach for predicting the structural and physical properties of DNA [84,85]. There are many other DNA studies available in the literature for describing the six helical systems [86] using atomic force microscopy. Also, a study has been done for the improved angle potential [87]. Importantly, in this study, the array of hexagonal six helix bundles is described in one-dimensional and two-dimensional cases. Furthermore, several studies of other biomolecular systems have been conducted and reported in the literature utilising the coarse-grained modelling approach [88–90]. Recently, the modelling of the coarse-grained structure of RNA and RNA-protein using the fluctuation matching method has been performed [91], making the same assumptions as reported in [49,79]. There are number of other investigations done on coarse-grained modelling of RNA for the prediction of tertiary structures [92–95]. In one of the earlier studies on the coarse-grained modelling of the three-dimensional structure of RNA, a single nucleobase has been approximated by five pseudo atoms [96]. Notably, the 688 experimentally determined structures of RNA have been used in this study for determining the force field parameters. The transformation of the all-atom model to the coarse-grained model was done utilising a typical three-bead approximation using the tcl scripting in the VMD software. Here we will describe the theoretical background of the coarse-grained modelling of the biomolecular system using the theory discussed in [91]. The coarse-grained potential for the RNA nanostructures can be expressed as:

$$V_{RNA} = V_{local} + V_{contact} + V_{excluded}, \tag{8}$$

where the local potential is the sum of the potential corresponding to bond lengths, bond angles and dihedral angles and can be expressed as [91]:

$$\begin{aligned} V_{local} = &\sum_{ibd} K_b(r_{ibd} - r^0_{ibd})^2 + \sum_{iba} K_\theta(\theta_{iba} - \theta^0_{iba})^2 \\ &+ \sum_{idih} K_\phi[1 - \cos(\phi_{idih} - \phi^0_{idih})] \\ &+ \frac{1}{2}K_\phi[1 - \cos 3(\phi_{idih} - \phi^0_{idih})], \end{aligned} \tag{9}$$

where r_{ibd} is the length of ibd-th virtual bond connecting ibd-th and (ibd + 1)-th coarse-grained particles; θ_{iba} is the iba-th virtual bond angle defined by iba-th, (iba + 1)-th, and (iba + 2)-th coarse-grained particles and ϕ_{idih} is the $idih$-th dihedral angle defined by $idih$-th, ($idih$ + 1)-th, ($idih$ + 2)-th, and ($idih$ + 3)-th coarse-grained particles. Further, the superscript '0' indicates the corresponding values of the variables in native structure and constants K are the parameters that modulate local stiffness of the RNA nanocluster.

Next, the potential coming from the nonlocal contact essential for structure-based modelling (taking into consideration only the natively contacting pairs (nat-con)) can be represented by:

$$V_{contact} = \sum_{i<j-3}^{nat-con} \epsilon_{go}\left[5\left(\frac{r^0_{ij}}{r_{ij}}\right)^{10} - 6\left(\frac{r^0_{ij}}{r_{ij}}\right)^{12}\right], \tag{10}$$

where r_{ij} is the distance between i and j atoms.

Furthermore, the non-native interaction (also known as the excluded term) for the coarse-grained potential is given by:

$$V_{excluded} = \sum_{i<j-3}^{non-native} \epsilon_{ex}\left(\frac{\mathrm{d}}{r_{ij}}\right)^{12}. \tag{11}$$

It is noteworthy to mention that the three-terms of Equation (8) (as described above) and their corresponding coefficient parameters (viz., K_b, K_θ, K_{phi}, ϵ_{go} and ϵ_{ex}) will be different for the different sets of structures. The equations for the potential described so far are only valid for those proteins in which the one-bead approximation is used. Certainly, in the development of coarse-grained models of the RNA and RNA-proteins, the expressions for the different terms in the coarse-grained potential will be different on the basis of their structures. Furthermore, the RNA molecule is a negatively charged system, due to which the RNA system attracts the opposite ions and is responsible of its folding character [97,98]. In order to account for this electronic charge of the RNA molecule and its consequences, the potential given by the Debye–Huckel model needs to be considered in the model as described in [91]. The existing coarse-grained models of RNA describe each RNA nucleotide with varying numbers of particles. Although, some of these earlier models are very coarse and highly simplified whereby only one or three pseudo-atoms were used to describe each RNA nucleotide, they are quite useful in prediction of 3D

RNA structures [99]. Recently, high resolution coarse-grained models of RNA molecules, such as HiRE-RNA [100–102], SimRNA [103], oxRNA [104], RNA-Martini models [99], etc., have also been explored for more accurately quantifying their overall behaviour along with simulating complex processes, viz., hybridisation, supercoiling and quadruplex formation [26,99,105]. More recently, a review related to recent advances in coarse-grained modelling of biomolecules along with their applications in biological systems have been presented in [73]. Furthermore, a data driven Bayesian statistical framework for the selection of coarse-grain water models has been recently provided in [106] that could serve as a powerful tool to refine, guide and critically assess molecular dynamics models. More details about these emerging methodological advances in machine learning and variational inference based Bayesian models can be found in [107,108].

2.3. Forced dynamics using molecular dynamics simulation

The steered molecular dynamics simulation is a computational modelling tool for studying mechanical properties of the molecular systems. The theory behind the steered molecular dynamics simulation has been described in [109,110]. During the steered molecular dynamics simulations, the constant velocity or a time-dependent external force is applied to the atom for generating the movement. The guiding potential in the steered molecular dynamics simulation generated due to the movement can be expressed as [111,112]:

$$V(r, t) = \frac{k}{2}[x(r) - x_0(t) - vt]^2, \tag{12}$$

where x_0 is the value of descriptor $x(r)$ in its initial state, t is time, k is the constant representing the strength of the applied force. After a predetermined time, the parameter x that is changing with constant velocity due to applied force is given by:

$$x(t) = x_0 + vt. \tag{13}$$

Further, the work done by this potential is represented by:

$$W = v\int_0^t -k[(x(r) - x_\lambda(t) - vt]\,\mathrm{d}t, \tag{14}$$

and hence the potential mean force is given by

$$F = -k_B T\langle \mathrm{e}^{-\beta W}\rangle, \tag{15}$$

where $\beta = 1/k_B T$ is the inverse temperature, k_B is the Boltzmann constant, T is the temperature of the system.

Recently the forced molecular dynamics simulation has been used to study several properties of the therapeutic proteins, including its absorption on a typical surfaces via protein unfolding [113–116]. The forced dynamics of biomolecular systems provide useful insights on the stability of the RNA nanoclusters. Further, the forced dynamics have been utilised for studying and understanding the stability of RNA nanorings in [117]. Importantly, in this study, the response of the elastic properties toward the forced dynamics has been studied in detail. A compressive (or expansive) force is applied to the 2310 atoms of the nucleic backbone, which is directed to (or from) the centre of mass of the nanoring by using steered dynamics tool available in the NAMD molecular dynamics software for quantifying their tensile or expansive elasticity. Rather, than applying a force directly, a uniform acceleration (ranging from 0.01 to 1.0 Å ps^{-2}) has been applied to each of the atoms of the nucleic backbone. Two cases were simulated: (a) quasi-linear (staircase-like) increment of the radial external force from zero to 1.0 Å ps^{-2} with an increment of 0.1 Å ps^{-2} and having a time interval of 100 ps between the increments, and (b) constant compressive/expansive force of 0.1 Å ps^{-2} for 1 ns. The principal findings of the forced dynamics are presented in Figure 2 in the context of the nanoring both for compressive and expansive forcing. Specifically, the radius of gyration for different situations has been presented. Furthermore, the elastic constant of the RNA nanoring has been quantified from the elastic response of the applied force on molecular system of RNA nanoring. In realistic applications, we need to consider large and more complex RNA systems to be used in the fields such as biomedical engineering. Therefore, the study of these properties in the longer RNA nanotubes will give a better insight into the application of this computational technique.

3. Modelling of RNA nanoscaffolds and different topological configurations

RNA nanoscaffolds are one of the important structures designed and constructed by exploiting the RNA nanoclusters. Here we will discuss some of these computationally developed RNA nanostructures that have been verified experimentally [17,118,119]. Note also that the stability of the RNA nanocubes has also been studied with respect to the length of the RNA building blocks utilising both experimental and computational approaches. The maximum stability of the nanocubes has been found for the structures that were built from a block of the RNA self-assembly containing 10 nucleotide. In Figure 3, the schematic of the self-assembly process of the RNA building blocks to form the RNA nanocubes has been presented. Furthermore, the optimisation for the best linking possibilities for construction of these RNA nanocubes has been described in Figure 4. Importantly, the three-dimensional elaborated structures from the corners are used to obtain the best possible junctions for the assembly of RNA nanocubes. The elastic network modelling was used for studying the properties of these nanocubes and modelling of the nanoscaffolds. Notably, the elastic network modelling is very common method for studying the characteristics of other biomolecular systems as well, such as the ribosomal tunnel and microtubules [120–122].

The experimental and theoretical modelling of the RNA nanoprisms has also been carried out by using the self-assembly of the conventional building blocks [123], as shown in Figure 5. The computational modelling of these structures has been performed using the folding of the two-dimensional structures and assembling the two RNA nanotriangles such that they are self-assembled to construct the three-dimensional shape. The computational modelling of the RNA nanotriangles has been described in [124]. The experimental and the theoretical study has also been performed on the homo-octameric nanoprisms from the self-assembly of RNA basic structures [125]. In

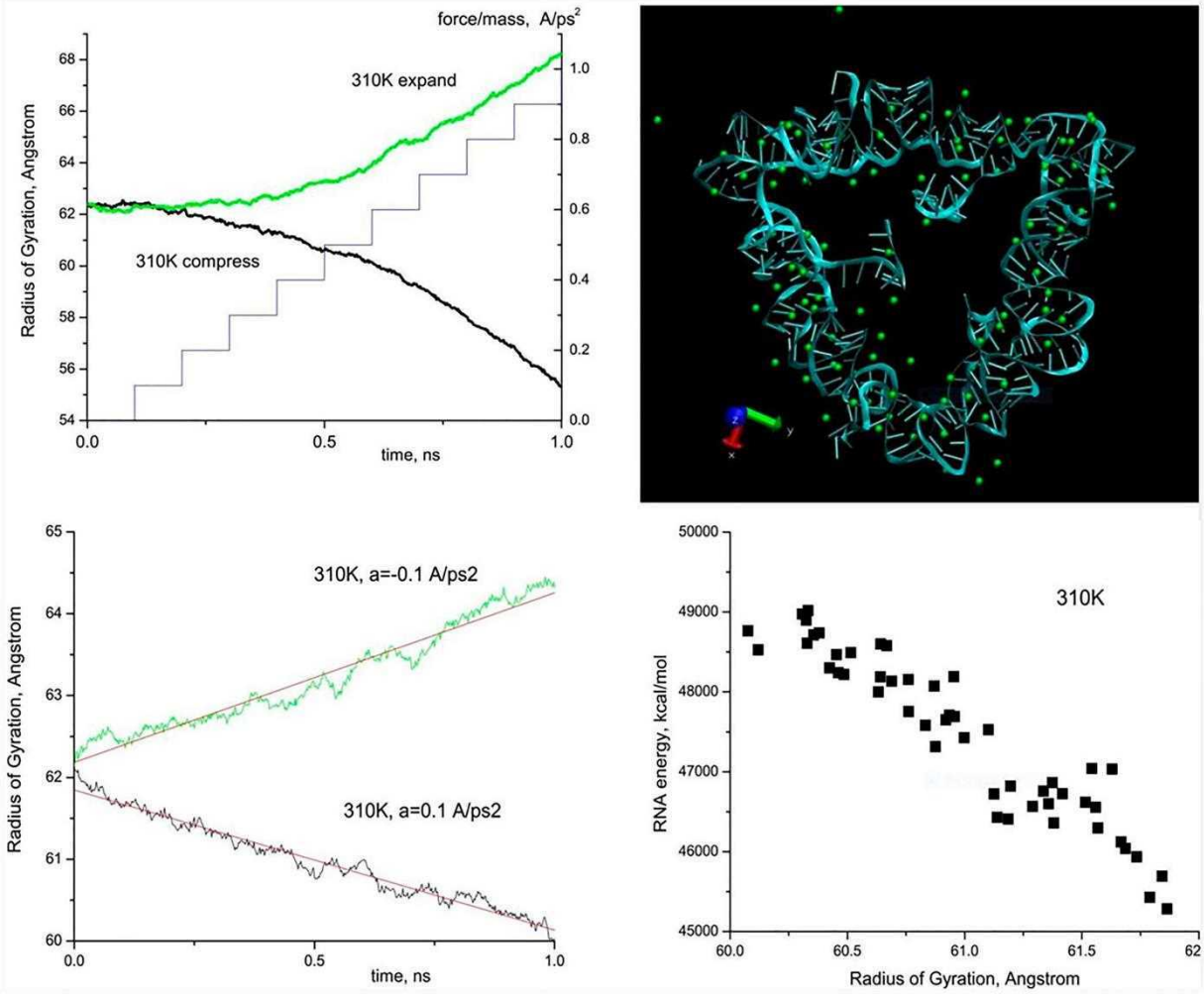

Figure 2. (Colour online) Computational modelling of the RNA nanoring using molecular dynamics simulation under external force to study the elastic response. Top (left): temporal variation of radius of gyration of the RNA nanoring (left y-axis) under the application of quasi-linearly increasing (staircase-like) radial external force (right y-axis); Top (right): snapshot of the RNA nanoring subjected to compressive force of 1.7 Å ps^{-2} at 310 K. Bottom (left): temporal variation of radius of gyration of the RNA nanoring under the application of the constant compressive/expansive force of 0.1 Å ps^{-2}; Bottom (right): dependence of the total energy of the RNA nanoring on its radius of gyration for the applied compressive force of 0.1 Å ps^{-2}. (This figure is reproduced with permission from [117].)

computational modelling of such structures, self-assembly of the RNA tiles has been constructed by joining the A-form RNA with the other different loops generated from the nucleic acid system. The square-shaped loops for constructing these tiles of RNA has been taken from the protein data bank (ID:3P59) [48]. Furthermore, the modelling of structures of the self-assembly of RNA building blocks to form the nano-triangle and nanosquares has been described in [126,127]. Further details about different topological architectures built from basic RNA building blocks, viz., 2D RNA triangles, squares and hexamers, and 3D RNA prisms, tetrahedrons, and dendrimers, along with other 4D structures can be found in a recent review in [3]. More recently, a versatile toolkit for programmable self-assembling of RNA-DNA hybrid nanoshapes as a flexible open platform architecture for different applications in nanotechnology, viz., molecular recognition, sensor and catalyst development, and studying protein interaction have been reported in [128]. This integration of RNA motifs (as architectural joints) and DNA building blocks (as functional modules) attest to the extraordinary robustness of the RNA-DNA hybrid framework for modification by addition of sequences, loops and conjugation sites. A coarse-grained RNA model RACER (RnA CoarsE-gRained) was developed by Bell et al. [129] for predicting the native structures for number of RNAs along with capturing RNA folding free energy. It was based on PDB structural statistics and experimental thermodynamic data, whereby the functional forms and parameters were determined by systematic optimisation against native structures and melting free energies of RNA molecules.

4. Modelling of RNA nanotubes

Nanotubes are defined as miniature materials that play a significant role in several exciting applications, such as nanotechnological, medical, biological and material sciences [130]. More recently, Li et al. [130] reports an experimental study related to the design, construction and characterisation of molecularly defined RNA nanotubes. Originally, the RNA nanorings and RNA nanotubes have been self-assembled for the first time using the computational technique in [29]. Later, several studies of RNA nanoclusters have been reported based on the molecular dynamics simulation. Importantly, the molecular

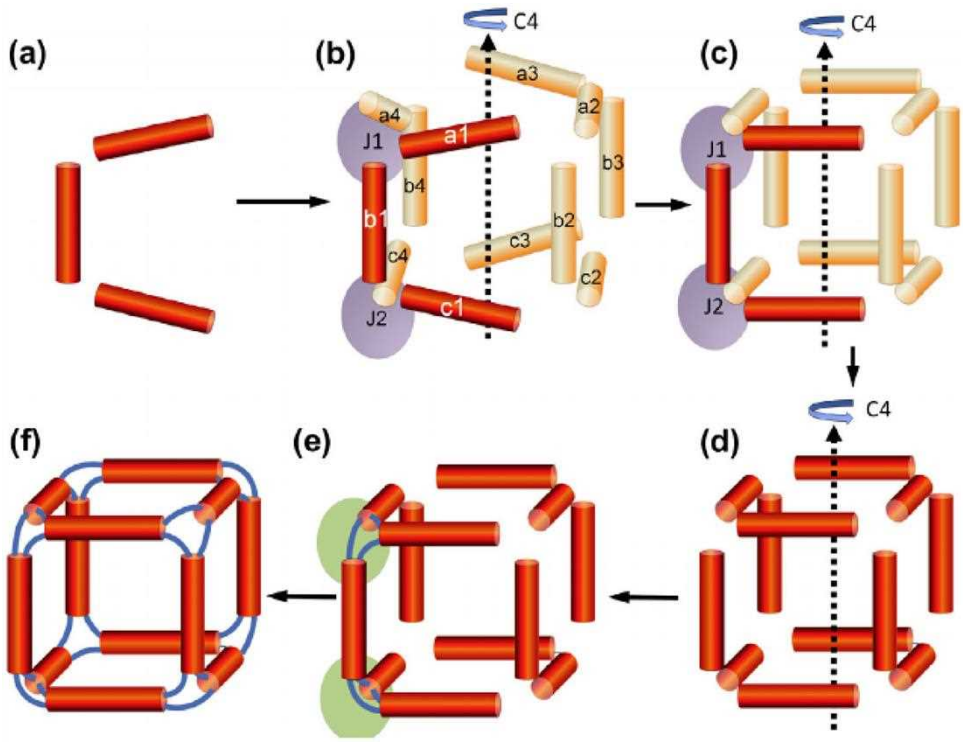

Figure 3. (Colour online) The schematic diagram for the modelling of the RNA nanocube from the RNA strands. The steps used for the modelling are represented in figures a to f. The RNA strands are helical and presented by the rod. These several rods while connected together make the RNA nanocubes. (This figure is reproduced with permission from [17].)

dynamics simulation technique has been used to study the properties of the RNA hexagonal nanorings constructed from the RNA building blocks, similar to the building blocks used in [29,117]. Using the atomistic model, an elaborate coarse-grained modelling of RNA nanoclusters has been performed in [79,117] utilising the Boltzmann inversion method. A three-bead approximation was used for coarse-grain modelling in such a way that the nucleobase, sugar group and the phosphate backbones are assigned with the first, second and third beads, respectively. For further advancement and development of the RNA nanotube, molecular dynamics simulation and coarse-grain modelling have been performed for studying their properties in [131–133]. Importantly, in [132] for the first time all-atom molecular dynamics simulations were performed on the RNA nanotubes made by connecting several hexagon-shaped RNA nanorings (up to 20 nm in size) for studying their structural properties, viz., root mean square deviation, radius of gyration and radial distribution function (RDF) in the physiological solutions. The RNA building blocks used for modelling the RNA nanotubes in these studies were RNAI/II complexes taken from the protein data bank (2bj2.pdb) [134], which are actually the sense and anti-sense plasmids responsible for controlling the ColE1 plasmid replication [135,136]. The CHARMM27 force field [137] implemented in the NAMD package [138] was used for performing the all-atom molecular dynamics simulations of RNA nantotubes solvated in a water box. The VMD [139] software was used for visualisation and analysis of the simulation results with different ring sizes. The size of the water box was chosen such that the distance between the nanocluster surface and the wall is slightly larger than the cutoff radius. To make the system neutral, appropriate number of sodium Na^+ and Cl^- ions were added. The RNA nanotubes system was simulated at constant temperature and constant pressure (NPT) ensemble utilising the NAMD software, whereby the temperature was controlled by using the Langavin method and the pressure was controlled by using the Nose–Hoover piston method [140,141]. The periodic boundary conditions were imposed in all three dimensions during the simulation. Further, the topotools available in the VMD was used for adding chemical bonds between the segments of the nanoclusters. Based on the same theory, the ion concentration dependence and the transport properties of RNA nanotubes have also been reported in [142–144].

Using molecular dynamics simulation, the radial distribution function for the RNA nanotube was calculated for the 4 coupled ring structure in the physiological solution of potassium chloride (KCL) by our group [142–144]. The model structure of the RNA nanotube immersed in the salt solutions is presented in Figure 6. Here the water is not presented for clearly visualising the presence of ions around the RNA nanotube. The calculated results for the radial distribution plots are presented in Figure 7. The position of the peaks observed in Figure 7 indicates the distance between the given species in the solution. The obtained results are reminiscent to the earlier all-atom molecular dynamics simulation studies conducted on the RNA nanoring [117]. In the radial distribution functions, the peaks observed from the plots in Figure 7 indicates the distance between the atoms taken in the radial direction. Furthermore, in the P-OH2 radial distribution plot, we see the multiple

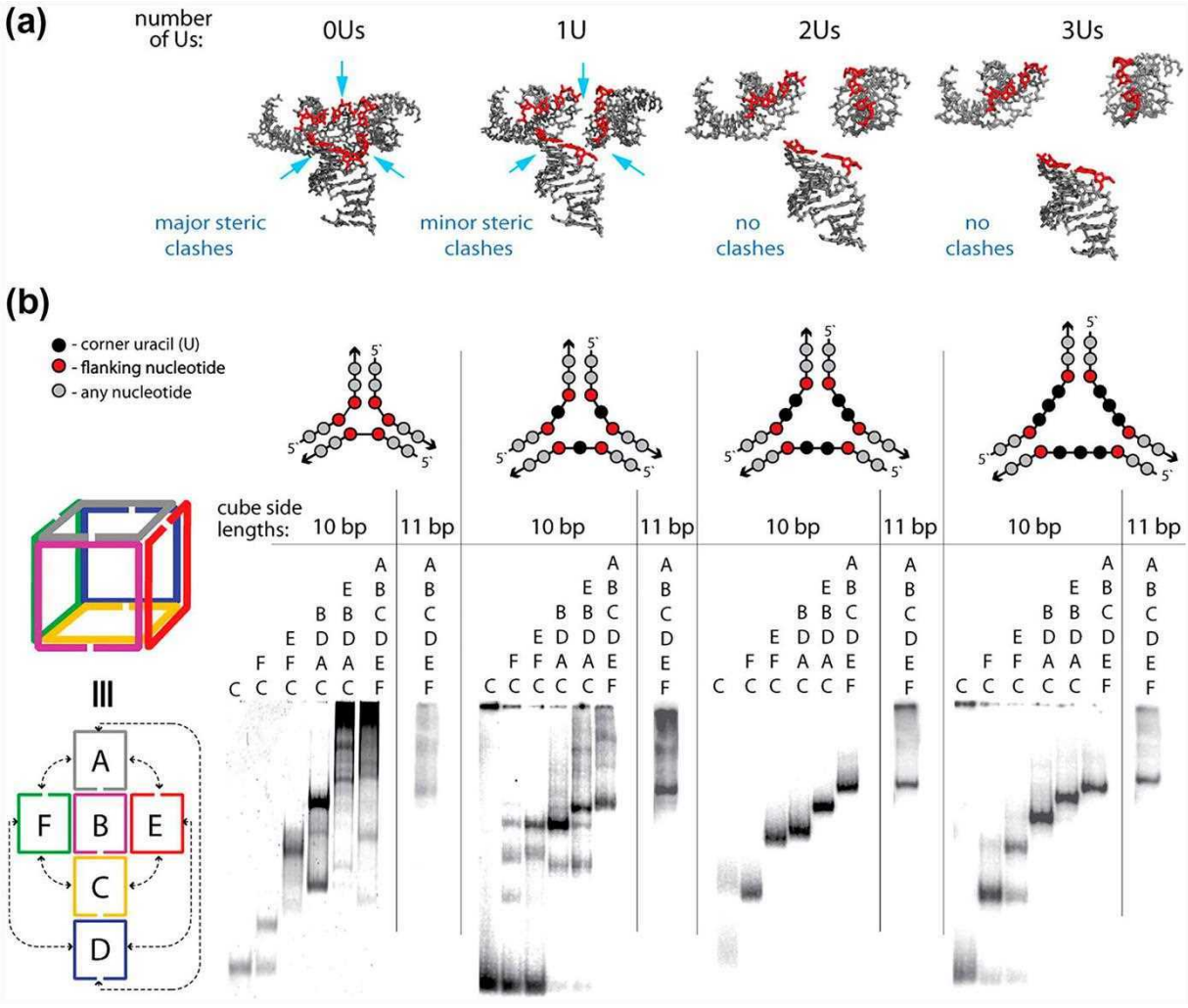

Figure 4. (Colour online) The computational models (a) and the experimental models (b) of the RNA nanocubes to show the effectiveness and schemes of the cube assembly to form the RNA nanoscaffold. (This figure is reproduced with permission from [17].)

peaks that provide the distance of the first, second and so on, solvation shell for the phosphorous atom in the RNA nanotube. Further, in another recent study, a coarse-grained model for 40 nm long RNA nanotubes (equivalent to 10 RNA nanorings connected in series) has been developed in [145], to systematically study their physical properties using all-atom molecular dynamics simulation on the three-bead approximation model of nanoring discussed earlier. The obtained results for the phosphorous-phosphorous (P-P) radial distribution functions of 1, 4, 5, and 10 ring RNA nanotubes have been presented in Figure 8. As depicted in Figure 8, the intensity of the radial distribution functions decreases with the increasing in number of RNA nanorings in the nanotube.

More recently, a study of hexagonal RNA nanotubes using several hundred nano-second long all-atom molecular dynamics simulations has been reported for studying the atomic structure, conformational change and mechanical properties in the presence of explicit water and ions [146]. The Nucleic Acid Builder (NAB) [147] program was used to build the initial structure of the RNA nanotubes using AMBERTools16 [148]. The closed structure of hexagonal nanotube was made from six double-stranded RNA connected by double crossover at different positions. Further, the two adjacent RNA helices (separated by 22.5 Å) were connected via two four-way Holliday junctions and the RNA strands were designed to have Watson-Crick complementary domains. The PDB structure initially built from NAB code was loaded in the xLEAP module of AMBERTools16 and the bonded and non-bonded interaction of the RNA nanotubes were defined by the leaprc.RNA.OL3 force field that includes some corrections to the AMBERff99 force field, in order to have structurally stable conformations over several microsecond long molecular dynamics simulations. The structure was then solvated using the TIP3P water model with the dimension of the solvation shell greater than 25 Å in all three directions. Furthermore, to neutralise the negative charge of the RNA backbone, an appropriate number of Na^+ ions were added using a potential grid of 1 Å. The Joung–Cheatham ion parameter set was used for describing the interaction of ions with waters and RNA nanotubes. Figure 9 shows the RNA nanotube structure solvated in aqueous solution. Importantly, in [146] two different structures of RNA nanotubes were used: (a) RNT1 that has identical crossover and nick design to the experimental design of the DNA nanotubes in [149,150] whereby the thymines are replaced by

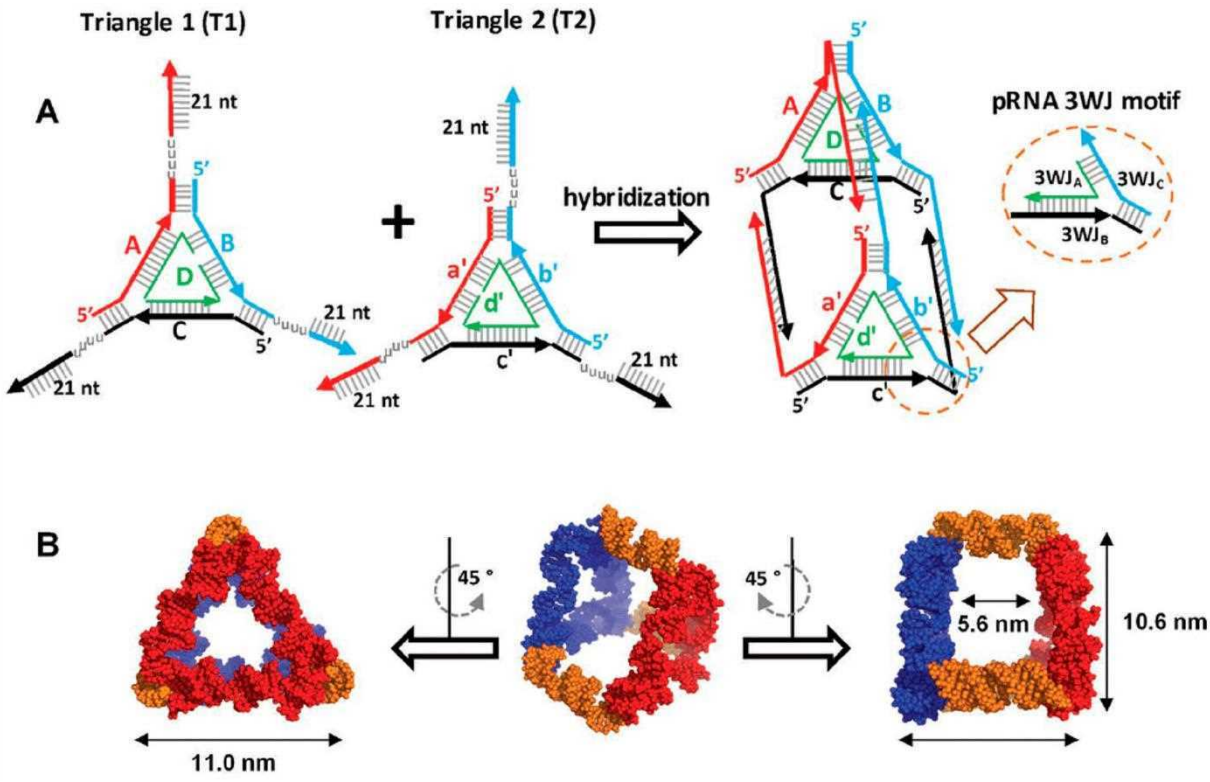

Figure 5. (Colour online) The experimental models (a) and computational models (b) of the RNA nanoprism to show the effectiveness and schemes of the triangular assembly to form the RNA nanoscaffold. (This figure is reproduced with permission from [123].)

uracils, and (b) RNT2 that was taken from the experimental RNA origami tube design by [151] whereby owing to the computational difficulties in simulating the large origami nanotubes only a portion of the nanotube was used. A 56 bp long RNT2 was used to make it symmetric in both sides in comparison to 57 bp long RNT1. All the simulations were performed using the parallel version of the PMEMD module of the AMBER software package and the VMD package was used for visualisation and generation of results. Figure 10 shows the instantaneous snapshots of the RNA nanotubes after 200 ns. As evident from Figure 10, the RNA nanotubes maintain a nice tubular structure over the simulation timescale. The RDF analysis of the phosphate-phosphate (P-P) and Na^+ around phosphate has been presented in Figure 11 that could be helpful for investigating the distribution of different ion groups around the RNA nanotubes. Recently, in another experimental study [152], the design and characterisation of RNA nanotubes formed by five distinct RNA strands have been presented. Importantly, with an average size of 45–90 MDa, the RNA nanotubes described in this study were the largest existing structured RNA assemblies.

The atomistic to continuum multiscale modelling approach is quite popular for bridging the two scales and predicting the elastic properties of carbon nanotubes [153–156] having similar physical structures as of RNA nanotubes. These atomistic to continuum multiscale approaches can be broadly classified into two categories: (a) those developed with a simultaneous (concurrent) implementation and (b) those developed with a serial (hierarchical) implementation [157]. The first group that couples 'critical', atomistically modelled regions (or a region) with their 'continuum' surroundings has received significant attention from quite some time [158–160]. Different variants of these methods range from the methodologies related to bridging-scale methods to various continuum-field theory, and from atomistic-scale finite element methods to matching multiscale simulations [161–164]. Some of these methods have been recently applied to biomolecules, such as DNA, collagen fibril proteins and microtubules [165–170] for studying their mechanical properties, but in a simplified setting that is far from challenges represented by realistic biological nanostructures. Moreover, the second group (hierarchical continuum-on-atomistic methods) has been less studied until recently [171]. More recently, an atomistic-based continuum multiscale model for studying the mechanical properties of RNA nanotubes has been presented in [161]. In this study, the optimised structure of self-assembled RNA nanoclusters was derived from the atomistic based molecular dynamic simulations for different ring sizes (viz., 5, 10, 20 and 30 rings), which was later approximated by the RNA nanotube considering a cylindrical hollow shell model for continuum calculations. The elastic properties of RNA nanotubes were then studied utilising linear constitutive stress-strain relations using both Dirichlet and Neumann boundary conditions.

5. Applications

In this section, we will discuss about different applications of RNA nanoclusters, primarily in the field of nanomedicine and nanobiotechnology.

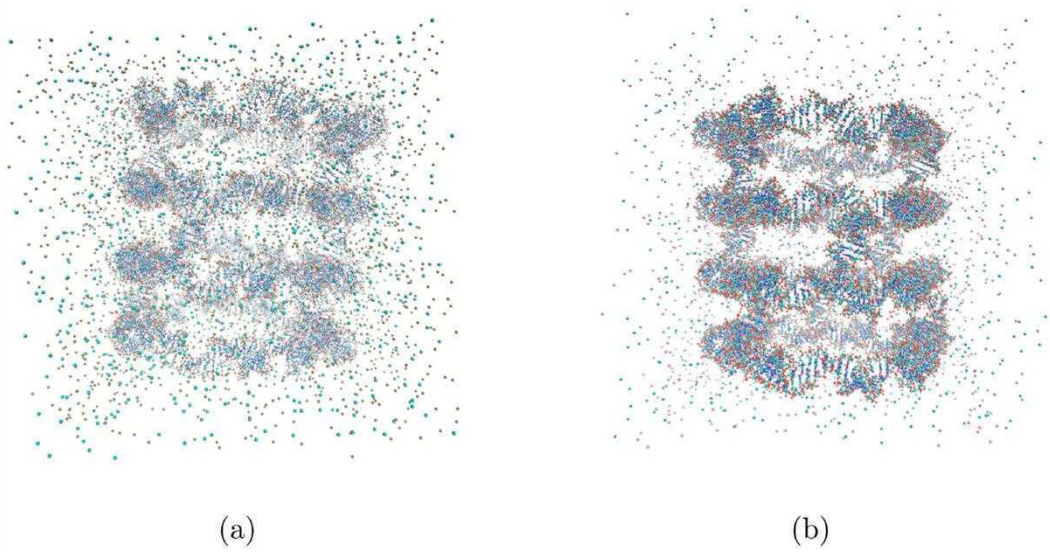

Figure 6. (Colour online) VMD generated structure of the RNA nanotube in physiological solutions (a) KCL (b) $MgCl_2$.

5.1. Nanodevices for medical imaging and other applications

Biocompatibility of the RNA self-assemblies makes them a very good candidate for different potential applications in medical imaging. This biocompatibility property of RNA can be accounted to the variable length of the RNA strand along with well-known base pairing in which the guanine with the cytosine and adenine with uracil are attracted to the hydrogen bonding. The application and compatibility of the nucleic nanoclusters for the nanodevice applications are described in extensive detail in some of the recent studies [172–183]. Furthermore, the application of the DNA-based nanodevices on the cell functioning, medical imaging and finding the gene expression has been extensively discussed in [184–195]. The RNA nanoclusters can also be used as the molecular logic gates and the single-strand RNA toeholds can be used for multiple split functionalities inside the human cell [196–204]. Some of the recent applications of the RNA nanoparticles in medical

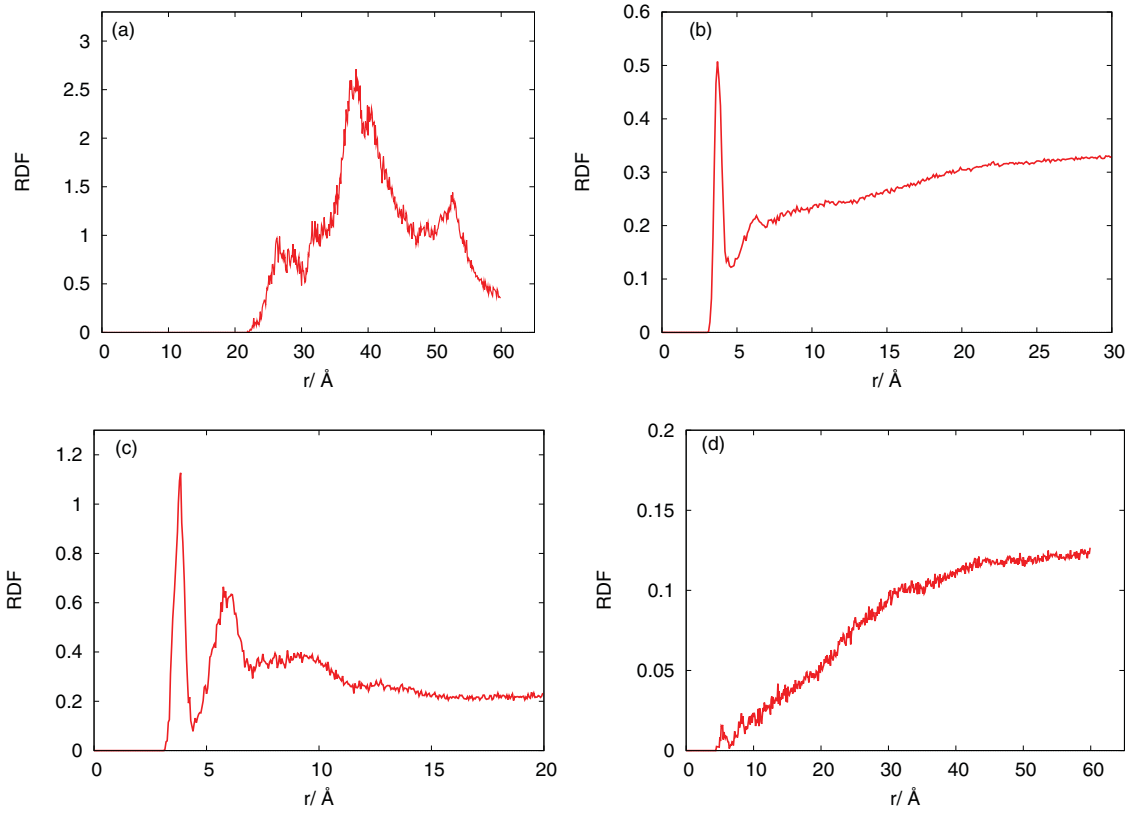

Figure 7. (Colour online) Radial distribution function for the RNA nanotube in the KCL solution (a) P-P (b) P-OH2 (c) P-K and (d) P-Cl.

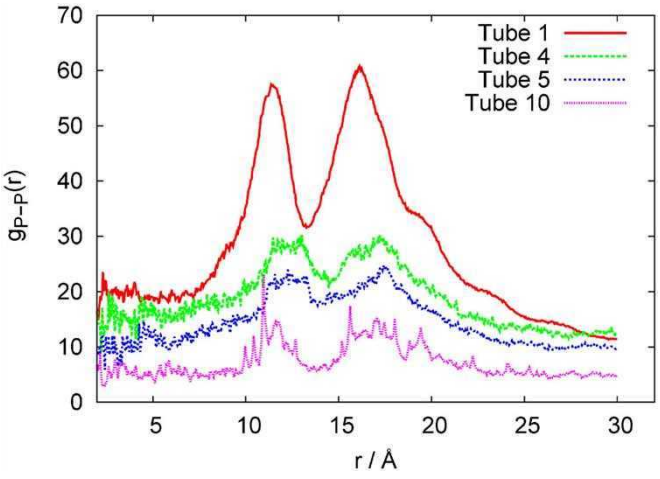

Figure 8. (Colour online) P-P Radial distribution functions for the coarse-grained models of 1-, 4-, 5-, and 10-ring RNA nanotube. (This figure is reproduced from [145] under the terms of the Creative Commons Attribution 4.0 International License, http://creativecommons.org/licenses/by/4.0/, Copyright © 1996-2020 Licensee MDPI, Basel, Switzerland.)

imaging has been provided in [205–208]. Several promising applications of the tetra-uracil RNA motifs via modelling of the triangular-shaped nanostructures using RNA, DNA and RNA/DNA mixtures have been provided in the field of nanotechnology and nanomedicine in [209]. More recently, nucleic acid-based probes have emerged as a promising platform and gained popularity for detecting and visualising a wide variety of intracellular analytes in live cells [177]. Such advancements have become possible owing to the several distinct

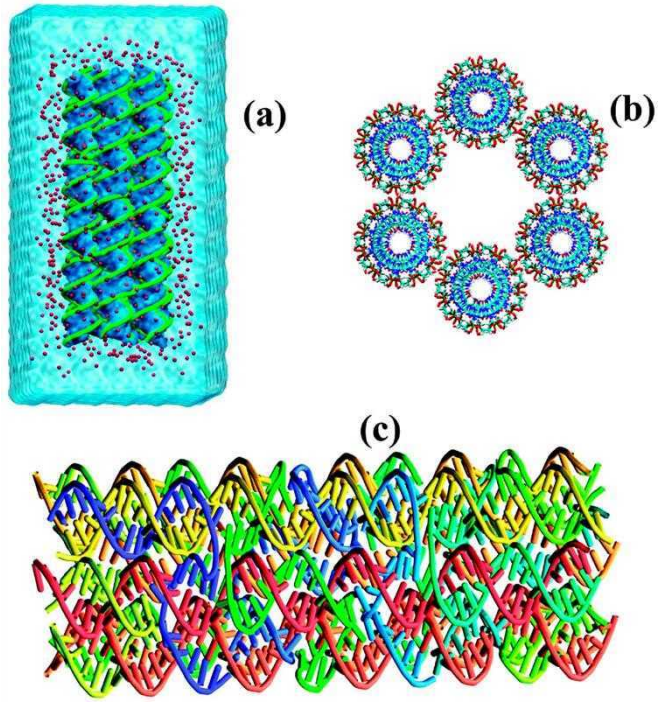

Figure 9. (Colour online) (a) Initial structure of the RNA nanotube immersed in a rectangular box of water where red dots represents Na^+ ion, (b) Top view of the hexagonal RNA nanotube system, and (c) Horizontally rotated view of the same system without water and ion. (This figure is reproduced with permission from [146].)

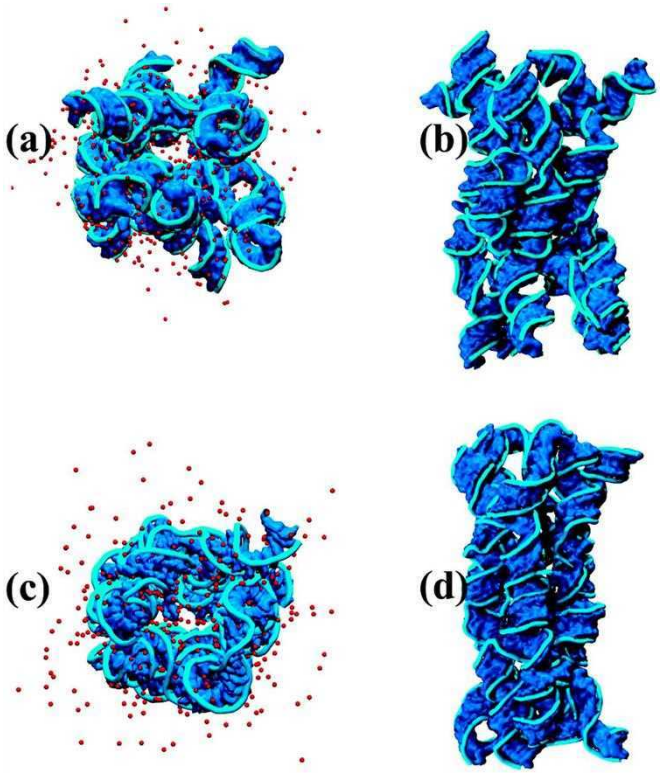

Figure 10. (Colour online) Snapshots of the system after 200 ns of simulation. Red dots represents Na^+ ion and water is not shown for clearly visualising the ions. (a) Top view and (b) side view of RNT1, and (c) top view and (d) side view of RNT2. (This figure is reproduced with permission from [146].)

advantageous properties of these nucleic acid-based probes. Importantly, these nucleic acid-based probes being biopolymers are biocompatible and nontoxic to cells, and can be utilised for visualisation of wide variety of targets inside living cells ranging from nucleic acids to ions, small molecules, proteins, etc. Recent advances in the field of live cell imaging using nucleic acid-based probes have been described in [177], clearly highlighting common probe design strategies, identification of different types of targets, current limitations and future perspectives. More recently, there has been a growing interest in developing image-guided vectors to detect RNA trafficking, endogenous gene expression and in vivo silencing [5]. For example, molecular beacon has become a popular in vitro detection technique to image intracellular RNA expression [210–212]. The applications of RNA nanoclusters have also been explored in fabrication and design of biomolecular memory and a bioinspired electronic nanodevice for information processing and computing, such as in the development of resistive random-access memory and field effect transistors [213,214].

5.2. Drug delivery

The RNA nanotubes and nanoscaffolds modelled from the self-assembly of the RNA nanocluster are found to be quite useful for drug delivery in treating cancer and other diseases. Recent advances in the field of RNA nanotechnology has allowed construction of different nanoscale shapes derived from the RNA-based functional moieties, viz., aptamers, riboswitches,

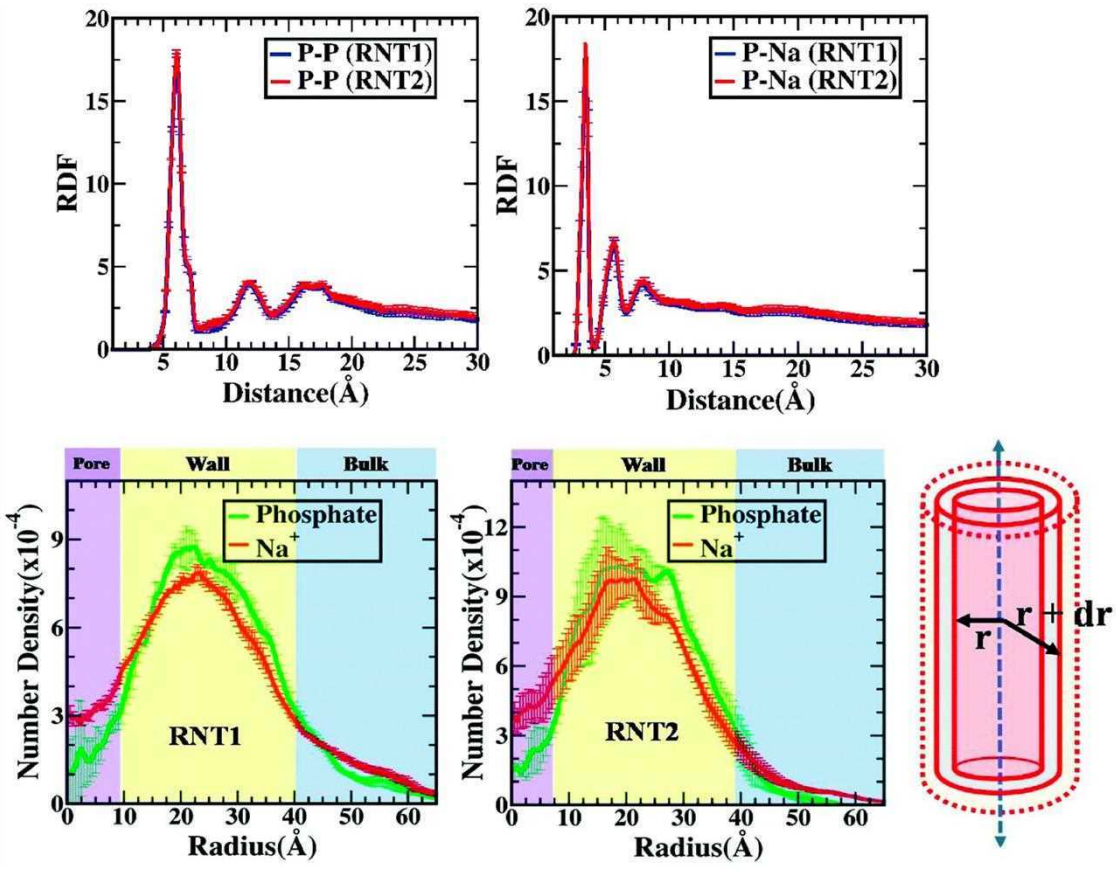

Figure 11. (Colour online) Radial distribution function of RNA nanotube for (a) phosphate-phosphate and (b) phosphate-Na^+ ion, and (c) Number density profile of the Phosphate and Na^+ ion along the radially outward direction. (This figure is reproduced with permission from [146].)

ribozymes, siRNAs, etc. which clearly highlights the current potential of the RNA nanoscaffolds for simultaneous delivering the specific therapeutics to the target tissue while controlling the stoichiometry and composition of the drug delivered [3,17,215–219]. Earlier works in this field have demonstrated the assembly of modular RNA units into different complex architectures, such as functional dimers, trimers, tetramers, pentamers, hexameric nanorings, heptamers, octameric squares, 1D and 2D arrays composed of filaments and tecto-squares, 3D supra-molecular RNA architectures, and several different cubic nanoscaffolds that are functionalised with aptamers and therapeutic siRNAs [17,29,42,43,47,117,118,220–223]. All these recent studies in the field of RNA nanotechnology suggest that the RNA nanoscaffolds have become promising candidates for therapeutic purposes. However, more extensive and detailed studies in this research direction are required for our better understanding of the existing RNA nano-constructs with the motive of further improvement in their design and fabrication which could be quite useful in its clinical translation in the field of nanomedicine. The computational modelling approach presented in earlier sections could be used to optimise the nanostructure design decisions and help predict the best experimental strategy. One such integrated computational and experimental study has been reported in [17] to optimise and characterise the cubic nanoscaffold designs. Moreover, previous in vivo study in a mice has demonstrated that RNA nanoscaffold displays favourable pharmacokinetic and pharmacodynamic profiles and is non-toxic [55,224]. Thus, taking the advantage of these favourable characteristics of RNA nanostructures, scientists have successfully exploited their usage as carriers or scaffolds to control cells function and fate. However, there still prevails significant barriers that needs to be overcome to utilise full potential of the field of RNA nanotechnology in future medicine. One of the major stumbling blocks in computational simulations (at any scale, from coarse-grained to QM/MM) is the actual delivery process of a drug molecule encased in the RNA nanostructure. At present, cellular uptake still represents the major issue in the RNA nanoparticles that can be only loaded with very small capacity of the drug [5]. More recently, the construction of biocompatible and biodegradable 3D RNA polygons have been reported that can potentially serve as RNA cages or containers to encapsulate large capacity of small molecule drugs. Another important challenge to be addressed is the intracellular RNA nanoparticle trafficking. Like other nanoparticles-based drug delivery platforms, RNA nanoparticles also enter cells through receptor-mediated endocytosisis which once sorted is transferred to late endosomes and lysosomes whereby these nanoparticle are trapped without reaching their intended target [5]. Although as reported earlier, the endosomal escape of RNA nanoparticle delivery using small 8 nt anti-miRNA LNA fragments was successful in cancer regression, the efficacy of endosomal escape of siRNA delivery via receptor-mediated endocytosis is relatively low [5,225,226]. Also, the

cellular endocytosis or internalisation pathways that govern subsequent intracellular processing and endosomal escape of RNA nanoparticles is not fully understood till date. A comprehensive review highlighting the key biophysical aspects of drug delivery systems and the importance of the computational modelling in designing rational design of nanoparticle-based drug delivery system with improved and optimised properties has been presented in [227,228]. More recently, a silico study utilising MARTINI force-filed has been reported in [229] that aims at exploring molecular features driving supramolecular characteristics of dendrimer-siRNA complexation in terms of assemble mechanisms and competition phenomena. Other molecular dynamics studies relevant to the binding and delivery of RNA nanoparticles can be found in [230–232]. Moreover, to date, most of the RNA nanostructures are very simple in geometric shapes and their sizes are even smaller than most of the natural functional RNA [233]. Therefore, there is a significant need of expanding the complexity of nanostructures by designing and constructing novel nanostructures that can be utilised in several exciting applications in the field of nanomedicines, such as drug delivery and disease treatments. Mathematical and computational modelling could be a powerful tool that can play a vital role in addressing aforementioned challenges and expanding the field of RNA nanotechnology.

More recently, an elaborated review on the RNA nanostructures (including RNA-protein complexes) and scaffolds for biotechnology applications has been presented in [233]. Further details on drug delivery applications of RNA nanoparticles have been discussed in the context of the treatment of several types of cancer in [234–236]. The modelling of different types of RNA nanoparticles for various applications has been reviewed in more details in the previous literature [237,238]. In the earlier review the application of the RNA nanotechnology in drug delivery, tissue engineering, delivery for the specific target, has been discussed [7,218,239,240]. Other exciting applications of the RNA self-assembly in drug delivery have been provided in [209,241,242]. Notably, RNA-based therapeutics, viz., siRNA, miRNA, aptamers, chemical ligands can be simply incorporated to the RNA nanoparticle scaffold by fusing the sequences that can be utilised for specific targeted drug delivery systems to significantly reduce the nanoparticle accumulation within healthy organs and off-target toxicity [3,5]. Specifically, there are two ways for delivering the drug to the target site. One is by making the RNA nanoclusters from the drug itself like siRNA and then inserting it into the human body. And, the other way is by attaching or enclosing the drug inside the RNA nanostructures and releasing them into the target cell for the specific therapy. Furthermore, the pharmacological profiles of the RNA nanoparticles can be tuned in vivo by controlling their shape, size and physiochemical properties for achieving optimal targeting and enhanced therapeutic outcomes [3]. Here we are only highlighting the most recently developed RNA nanoclusters for delivering siRNA that can be useful for treating different types of cancers, specifically, the two-in-one RNA interference terminology that is capable of silencing the two messenger RNAs [235,243]. The procedures for the production of these kinds of the RNA nanoparticles have been described in Figure 12. In this figure, the self-assembling process of Folate DNA Cholesterol complex systems that is capable of delivering two kinds of drugs at the same cancerous cell has been demonstrated.

5.3. RNA interference and gene silencing

RNA interference (RNAi) is the process by which the expression of a gene is modulated utilising a short double-stranded RNA sequences having typical length of 21–23 nucleotides [4–6,244]. Mainly, there are two general molecules of RNAi: (a) miRNA that are endogenous to cells and can target multiple genes, and (b) siRNA that are mostly artificial sequences designed to target a specific messenger RNA (mRNA), and theoretically, any known mRNA sequence can be targeted using both of them. Once the miRNA and siRNA is binded to the target mRNA transcript, post-transcriptional gene silencing can be attained by two distinct mechanisms, viz., translational repression and degradation of mRNAs with imperfect complementarity, and sequence specific cleavage of perfectly complementarily mRNAs [244,245]. The specific delivery of siRNA to cancer receptor targets utilising the potential of pRNA platform for silencing the particular genes has been previously demonstrated in treating different types of cancers, such as breast, brain, prostate, cervical, gastric, nasopharyngeal carcinoma, leukaemia and ovarian cancer, as well as viral infections [3,55,225,226,246]. The mathematical and computational modelling approach can be utilised for advancing this RNAi field of research by rationally designing RNA nanoparticles for different needs, such as for harbouring identical siRNAs targeted to the same locus on one gene, different siRNAs targeted to different loci on one gene and different siRNAs targeted to different genes [32,55,247,248].

Recently, on August 2018 the US Food and Drug Administration (FDA) has approved the first RNAi based drug ONPATTRO (patisiran), an siRNA that is administered into the liver for treatment of hereditary transthyretin amyloidosis (hATTR) with polyneuropathy [6]. Apart from ONPATTRO success, there are approximately 40 chemically synthesised siRNAs that are undergoing clinical trials with many more on the way for treating other diseases apart from cancer, such as cardio-metabolic diseases, rare or genetic diseases, ophthalmological diseases, etc [4]. The FDA approval of this therapy has marked the new era in the RNAi therapy field. More recently, a review paper highlights the key advances in the design and development of RNAi drugs and its prospects for future applications [6]. Currently, CRISPR (clustered regularly interspaced short palindromic repeats) based RNA-targeting systems have attracted much attention owing to its significant potential to specifically edit, add or remove genes from a genome, as demonstrated in the suppression of hepatitis B virus in chronically infected cells [5,249–253]. Furthermore, the application of gene silencing through RNAi has also gained interest in the field of organ transplantation, preservation and re-conditioning [245,254–256]. The potential of RNAi application in the field of organ transplantation has been thoroughly reviewed in [254], highlighting previously reported RNAi studies for targeting genes related to ischemiare-perfusion injury (IRI) in liver, kidney, lung and heart transplantation. In an another recent study [257], a nanotube-based platform was developed for direct

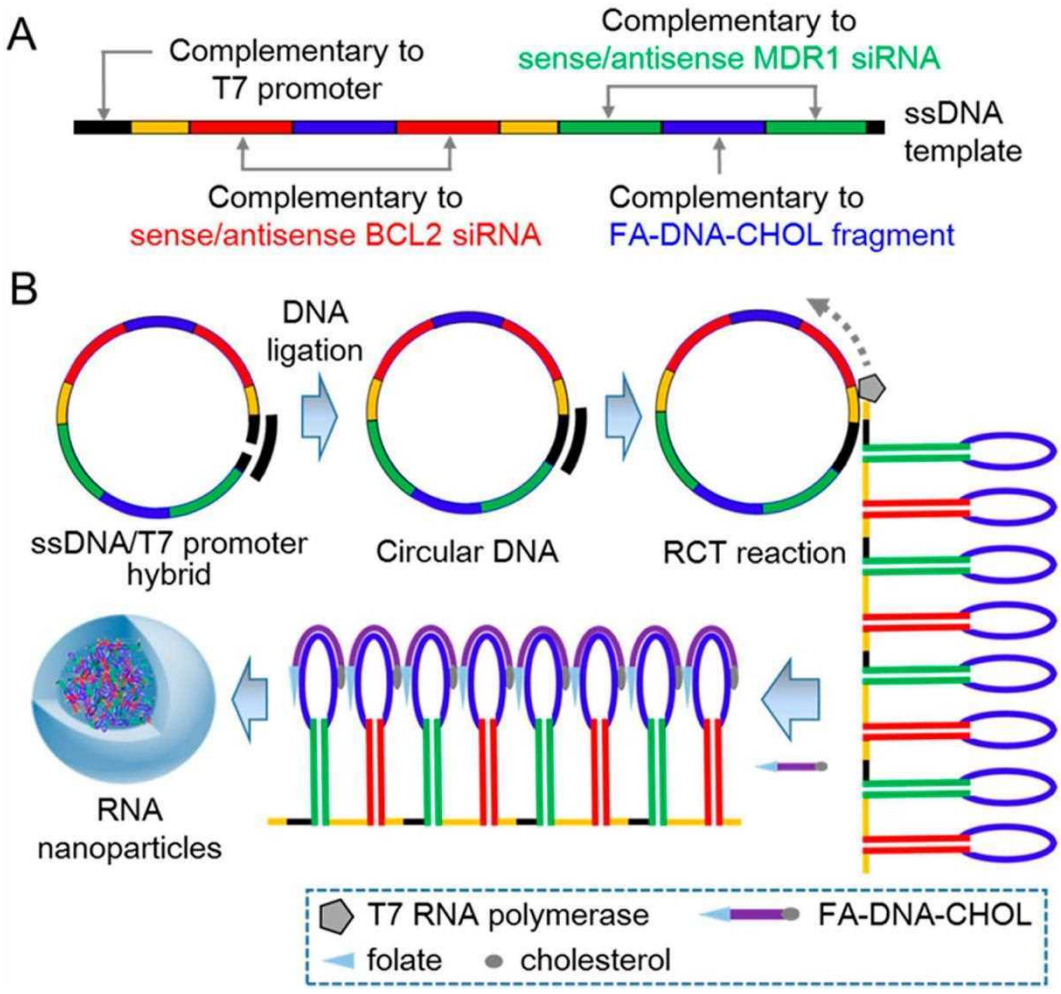

Figure 12. (Colour online) Demonstration of the synthesis of RNA nanoparticles as a two-in-one siRNA delivery system [235]. (This image is reproduced under the terms of the Creative Commons Attribution 4.0 International License (http://creativecommons.org/licenses/by/4.0/), Copyright © 2020, Springer Nature.)

delivery of siRNA in intact plant cells. This study demonstrated the efficacy of the nanotubes in successful intracellular delivery of siRNA for silencing the endogenous genes, clearing highlighting plethora of applications in the field of plant biotechnology relying basically on RNA delivery to intact cells. More recently, utilising molecular dynamics simulation a new truncated tetrahedral RNA nanoparticle was developed based on a core scaffold that displays an enhanced characteristics for RNAi-substrate delivery by increasing functional capacity, cellular uptake and RNAi efficacy of Dicer substrate siRNAs [258]. Thus, clearly highlighting that the structure of RNA scaffolds tremendously influences a nanoparticle's downstream RNAi-efficacy.

5.4. Disease treatments and cytotoxicity issues

Several nanoparticles platforms, viz., liposomes, polymers, viral nanoparticles, dendrimers and inorganic nanoparticles have been extensively developed and studied in the past decades for improving the performance of therapeutic modalities [5,259–264]. Although, these sub-micron-sized platform show tremendous potential in treating different diseases, their non-specific accumulation and retention away from the target site in the healthy vital organs still remains the major obstacle, apart from their high production cost, unstable thermodynamic and chemical properties, and lack of controlled-release mechanisms [5]. Moreover, their low specificity reduces the amount of adequate nanoparticles deposition within the diseased cells, thereby increasing the toxic side-effects. Most of these adverse effects are directly related to nanoparticles heterogeneity, aggregation, dissociation, unfavourable pharmacokinetic and pharmacodynamic profiles, and difficulties associated in penetrating the surrounding biological barriers of diseased cells [5]. Recent advances in the field of RNA-based therapy have shown that RNA nanoparticles may address several aforementioned major hurdles in the field of nanomedicine for cancer therapy, viral infections and eye disease [5,225,226,246,265–269]. Unlike conventional nanoparticles, RNA-based nanoparticles are highly selective, bio-compatible, non-toxic and have a low risk of off-target binding [270,271]. In addition, the RNA synthesis and production has become relatively rapid and cost-effective due to recent advances and boom in the field of RNA nanotechnology in past few years [55,271].

The nucleic acids have a very important contribution on the efficacy of radiotherapy and chemotherapy for cancer treatment as described in [272–274]. The identification of a certain kind of the RNA can also be done using nucleic acid metal nanoclusters [275]. Furthermore, nanoparticles can be used

as a sensitiser to increase the effectiveness of the radiotherapy [276]. The nanoparticles are usually inserted to the local environment of the cancerous tissue using drug delivery mechanisms. Furthermore, the nanotechnology has improved the delivery of the interfering RNA to the body for the cancer treatment [57,277]. The hydrophobic effect is a very important phenomenon that can be taken as a parameter to measure the accumulation of the drug at different organs of the body when delivered. The study of these properties has been performed for quantifying the accumulation of RNA nanoparticle conjugated with the different chemicals [278]. Accordingly, hydrophobicity was found to be changing with accumulation of the drug and is very useful for studying several characteristic properties of RNA nanoparticles such as cytotoxicity [278]. There are several kinds of RNA nanoclusters that can be used for the targeted drug delivery for treating cancer, such as magnetic nanoflowers and other macromolecules used for tumour-targeted therapy [279–281]. In treatment of human prostate cancer, the RNA aptamers are also being used as the probe during the screening process using the 3D Cell SELEX (systematic evolution of ligands by an exponential enrichment) procedure [282]. Moreover, tens of cell-internalising RNA aptamers that can be incorporated into RNA nanoparticles by sequence fusion are available for targeting specific cell surface receptors, viz., glioblastoma, breast cancer, prostate cancer, ovarian cancer, colon cancer, lymphoma cells, and viral infected cells (e.g. HIV) [5]. Furthermore, RNA aptamers are also used for the treatment of neurological disorders, such as multiple sclerosis, Alzheimer's disease, Parkinson's disease and stroke. RNA nanoparticles have also shown considerable promise for targeting cancer metastasis, which is hard to target owing to the spread of tumorous cells to distant body organs and lymph nodes [5]. RNA nanoparticles have shown a considerable potential to serve as vaccine adjuvant and immunotherapeutic reagent [3,5]. Recent studies highlighting the application of the RNA nanoparticles in treating different types of cancer has been provided in [283–286].

5.5. RNA structures with AI-based methods and other applications of data-driven technologies

The function and structures of RNA are mainly studied by predicting RNA secondary (not tertiary) structure from its primary structure. This is due to the difficulties associated with the direct prediction of very complex RNA tertiary structure (that even lacks effective representation) from primary structure of RNA. At present, although some RNA secondary structures can be obtained experimentally (e.g. X-ray crystallography, nuclear magnetic resonance (NMR) and cryogenic electron microscopy), these methods are not effective for all RNA molecules and are quite tedious, expensive and inefficient, specially for large structures [287–289]. Thus, computational methods provides a viable alternative for accurately and efficiently predicting the secondary structures of RNA that is quite essential for modelling RNA structures, as well as understanding their functional mechanisms [33,290–300]. Modern approaches for prediction of the RNA secondary structure are mainly based on thermodynamics principle based minimum free energy algorithm, whereby an iterative method is used to find the optimal folding state of RNA for meeting the minimum energy requirements or other constraints [288,301]. However, this approach is more accurate for predicting the secondary structure of shorter sequence of RNA and considerable deviations have been found in longer sequence of RNA due to fluctuations in the biopotential energy balance, as elaborated in [288]. Currently, the RNA secondary structure can be predicted by two main types of algorithms: (a) deterministic dynamic programming [302–306], and (b) comparative sequence analysis methods [307–309].

Furthermore, there has been a rapid surge in the application of artificial intelligence methods in different fields of research. Reasonable results have been reported from the previously available studies in the literature for predicting the secondary structure of RNA utilising artificial intelligence learning algorithms, viz., genetic algorithm, neural network algorithm, support vector machine algorithm, etc. [288,310–312]. However, these algorithms were still used only on the small samples. Therefore, there is high need of developing fast and accurate algorithms for the prediction of RNA secondary structure design that could provide boost to this exciting field of RNA engineering. More recently, deep learning methods [313] have emerged and made a remarkable progress in the field of artificial intelligence, especially in sequence modelling, such as in the analysis of sequential speech signals, video frames and natural language texts [288,301]. These deep learning methods possess a significant potential for extracting the effective and implicit features in the large-scale data through deep-seated networks and using these features for constructing effective prediction models. The deep learning methods have already made a great breakthroughs in the field of prediction of protein secondary structure [314]. More recently, Zhang et al. [288] proposed a novel computational method for prediction of RNA secondary structure utilising a convolutional neural network model combined with a dynamic programming method for improving the accuracy of prediction with large-scale RNA sequence and structure data. The reported results of this study indicate that the proposed model has a 30 % higher prediction success rate as compared to other mainstream algorithms currently in use. Other recent applications of deep learning algorithms in prediction and design of RNA secondary structures can be found in [289,301,315–317].

6. Conclusions

In this review article, the current state-of-the-art developments in the field of computational and mathematical modelling of the RNA nanoclusters have been provided. Notably, molecular dynamics simulation, coarse-grain modelling and atomistic-to-continuum modelling approaches used in RNA nanotechnology have been highlighted. Most recent studies in the modelling of RNA nanoscaffolds and other topological configurations derived from the self-assemblies of RNA building blocks have been thoroughly discussed. Main focus is on the computationally derived structure of RNA nanorings, nanoprisms and nanotubes, owing to there huge potential in the field of drug delivery, cancer therapy, gene silencing, etc. We have also discussed the potential application of the RNA nanoclusters in synthetic biology, materials science and nanomedicine.

Acknowledgments

Authors are grateful to the NSERC and the CRC Program for their support. This work was made possible by the facilities of the Shared Hierarchical Academic Research Computing Network (SHARCNET:www.sharcnet.ca) and Compute/Calcul Canada. The authors are grateful to Dr P. J. Douglas Roberts for helping with technical SHARCNET computational aspects. RM is also acknowledging the support of BERC 2018-2021 program, the Spanish Ministry of Science, Innovation and Universities through the BCAM Severo Ochoa accreditation SEV-2017-0718, and the Basque Government fund Artificial Intelligence in BCAM EXP. 2019/00432.

Disclosure statement

No potential conflict of interest was reported by the author(s).

ORCID

Roderick Melnik http://orcid.org/0000-0002-1560-6684
Sundeep Singh http://orcid.org/0000-0002-8342-1622

References

[1] Guo P. The emerging field of RNA nanotechnology. Nat Nanotechnol. 2010;5(12):833.
[2] Guo P, Haque F. RNA nanotechnology and therapeutics: methods and protocols. New York: Humana Press, Springer; 2015.
[3] Haque F, Pi F, Zhao Z, et al. RNA versatility, flexibility, and thermostability for practice in RNA nanotechnology and biomedical applications. Wiley Interdiscip Rev RNA. 2018;9(1):e1452.
[4] Weng Y, Xiao H, Zhang J, et al. RNAi therapeutic and its innovative biotechnological evolution. Biotechnol Adv. 2019;37(5):801–825.
[5] Jasinski D, Haque F, Binzel DW, et al. Advancement of the emerging field of RNA nanotechnology. ACS Nano. 2017;11(2):1142–1164.
[6] Setten RL, Rossi JJ, Han Sp. The current state and future directions of RNAi-based therapeutics. Nature Rev Drug Discovery. 2019;18(6):421–446.
[7] Li M, Zheng M, Wu S, et al. In vivo production of RNA nanostructures via programmed folding of single-stranded RNAs. Nat Commun. 2018;9(1):1–9.
[8] Kuimelis RG, McLaughlin LW. Mechanisms of ribozyme-mediated RNA cleavage. Chem Rev. 1998;98(3):1027–1044.
[9] Boero M, Terakura K, Tateno M. Catalytic role of metal ion in the selection of competing reaction paths: a first principles molecular dynamics study of the enzymatic reaction in ribozyme. J Am Chem Soc. 2002;124(30):8949–8957.
[10] Martick M, Scott WG. Tertiary contacts distant from the active site prime a ribozyme for catalysis. Cell. 2006;126(2):309–320.
[11] Scott WG. Ribozymes. Curr Opin Struct Biol. 2007;17(3):280–286.
[12] Breaker RR. Riboswitches and the RNA world. Cold Spring Harb Perspect Biol. 2012;4(2):a003566.
[13] Ha M, Kim VN. Regulation of microRNA biogenesis. Nat Rev Mol Cell Biol. 2014;15(8):509–524.
[14] Jasinski DL, Li H, Guo P. The effect of size and shape of RNA nanoparticles on biodistribution. Mol Ther. 2018;26(3):784–792.
[15] Resnier P, Montier T, Mathieu V. A review of the current status of siRNA nanomedicines in the treatment of cancer. Biomaterials. 2013;34(27):6429–6443.
[16] Jedrzejczyk D, Gendaszewska-Darmach E, Pawlowska R, et al. Designing synthetic RNA for delivery by nanoparticles. J Phys Condens Matter. 2017;29(12):123001.
[17] Afonin KA, Kasprzak W, Bindewald E. Computational and experimental characterization of RNA cubic nanoscaffolds. Methods. 2014;67(2):256–265.
[18] Wolter AC, Weickhmann AK, Nasiri AH. A stably protonated adenine nucleotide with a highly shifted pKa value stabilizes the tertiary structure of a GTP-binding RNA aptamer. Angew Chem Int Ed. 2017;56(1):401–404.
[19] Cerchia L, de Franciscis V. Targeting cancer cells with nucleic acid aptamers. Trends Biotechnol. 2010;28(10):517–525.
[20] Bunka DH, Platonova O, Stockley PG. Development of aptamer therapeutics. Curr Opin Pharmacol. 2010;10(5):557–562.
[21] Sundaram P, Kurniawan H, Byrne ME. Therapeutic RNA aptamers in clinical trials. Eur J Pharm Sci. 2013;48(1–2):259–271.
[22] Chushak YG, Martin JA, Chávez JL, et al. Computational design of RNA libraries for in vitro selection of aptamers. In: Artificial riboswitches. Springer; 2014. p. 1–15.
[23] Rozenblum GT, Lopez VG, Vitullo AD, et al. Aptamers: current challenges and future prospects. Expert Opin Drug Discov. 2016;11(2):127–135.
[24] Chushak Y, Stone MO. In silico selection of RNA aptamers. Nucleic Acids Res. 2009;37(12):e87.
[25] Albada HB, Golub E, Willner I. Computational docking simulations of a DNA-aptamer for argininamide and related ligands. J Comput Aided Mol Des. 2015;29(7):643–654.
[26] Cruz-León S, Vázquez-Mayagoitia A, Melchionna S, et al. Coarse-grained double-stranded RNA model from quantum-mechanical calculations. J Phys Chem B. 2018;122(32):7915–7928.
[27] Sun LZ, Zhang D, Chen SJ. Theory and modeling of RNA structure and interactions with metal ions and small molecules. Annu Rev Biophys. 2017;46:227–246.
[28] Miao Z, Westhof E. RNA structure: advances and assessment of 3D structure prediction. Annu Rev Biophys. 2017;46:483–503.
[29] Yingling YG, Shapiro BA. Computational design of an RNA hexagonal nanoring and an RNA nanotube. Nano Lett. 2007;7(8):2328–2334.
[30] Sajja S, Chandler M, Fedorov D, et al. Dynamic behavior of RNA nanoparticles analyzed by AFM on a mica/air interface. Langmuir. 2018;34(49):15099–15108.
[31] Yang Xd, Melnik RV. Effect of internal viscosity of polymeric fluids under strong extensional flows. Chinese J Polymer Sci. 2009;27(02):189–193.
[32] Yang XD, Mahapatra DR, Melnik RV. Simulation of RNA silencing pathway for time-dependent transgene transcription rate. AIP Conference Proceedings; Vol. 952, American Institute of Physics; 2007. p. 229–237.
[33] Yesselman JD, Eiler D, Carlson ED, et al. Computational design of three-dimensional RNA structure and function. Nat Nanotechnol. 2019;14(9):866–873.
[34] David S, Marchais H, Hervé-Aubert K, et al. Use of experimental design methodology for the development of new magnetic siRNA nanovectors (MSN). Int J Pharm. 2013;454(2):660–667.
[35] David S, Marchais H, Bedin D. Modelling the response surface to predict the hydrodynamic diameters of theranostic magnetic siRNA nanovectors. Int J Pharm. 2015;478(1):409–415.
[36] Dim N, Perepelyuk M, Gomes O, et al. Novel targeted siRNA-loaded hybrid nanoparticles: preparation, characterization and in vitro evaluation. J Nanobiotechnology. 2015;13:61.
[37] Hatakeyama H, Wu S, Mangala L, et al. Assessment of in vivo siRNA delivery in cancer mouse models. In: Feng Y, Zhang L, editors. Long non-coding RNAs. New York: Springer; 2016. p. 189–197. (Methods in Molecular Biology; 1402).
[38] Pramanik A, Laha D, Dash SK. An in-vivo study for targeted delivery of copper-organic complex to breast cancer using chitosan polymer nanoparticles. Materials Sci Eng C. 2016;68:327–337.
[39] Hilder TA, Hill JM. Modeling the loading and unloading of drugs into nanotubes. Small. 2009;5(3):300–308.
[40] Davis D, Akhtar U, Keaster B. Challenges and potential for RNA nanoparticles (RNPs). J Biomed Nanotechnol. 2009;5(1):36–44.
[41] Afonin KA, Danilov EO, Novikova IV, et al. TokenRNA: a new type of sequence-specific, label-free fluorescent biosensor for folded RNA molecules. Chembiochem. 2008;9(12):1902–1905.
[42] Khaled A, Guo S, Li F. Controllable self-assembly of nanoparticles for specific delivery of multiple therapeutic molecules to cancer cells using RNA nanotechnology. Nano Lett. 2005;5(9):1797–1808.

[43] Shu D, Shu Y, Haque F. Thermodynamically stable RNA three-way junction for constructing multifunctional nanoparticles for delivery of therapeutics. Nat Nano. 2011;6(10):658–667.
[44] Novikova IV, Hassan BH, Mirzoyan MG. Engineering cooperative tecto-RNA complexes having programmable stoichiometries. Nucleic Acids Res. 2011;39(7):2903–2917.
[45] Ohno H, Kobayashi T, Kabata R. Synthetic RNA-protein complex shaped like an equilateral triangle. Nat Nano. 2011;6(2):116–120.
[46] Grabow WW, Zakrevsky P, Afonin KA. Self-assembling RNA nanorings based on RNAI/II inverse kissing complexes. Nano Lett. 2011;11(2):878–887.
[47] Afonin KA, Kireeva M, Grabow WW. Co-transcriptional assembly of chemically modified RNA nanoparticles functionalized with siRNAs. Nano Lett. 2012;12(10):5192–5195.
[48] Dibrov SM, McLean J, Parsons J. Self-assembling RNA square. PNAS. 2011;108(16):6405–6408.
[49] Nasalean L, Baudrey S, Leontis NB. Controlling RNA self-assembly to form filaments. Nucleic Acids Res. 2006;34(5):1381–1392.
[50] Giljohann DA, Seferos DS, Patel PC. Oligonucleotide loading determines cellular uptake of DNA-modified gold nanoparticles. Nano Lett. 2007;7(12):3818–3821.
[51] Stefaniak F, Chudyk EI, Bodkin M. Modeling of ribonucleic acid-ligand interactions. WIREs Comput Mol Sci. 2015;5(6):425–439.
[52] Kimoto M, Yamashige R, Matsunaga Ki. Generation of high-affinity DNA aptamers using an expanded genetic alphabet. Nat Biotech. 2013;31(5):453–457.
[53] Lawrence C, Vallée-Bélisle A, Pfeil SH. A comparison of the folding kinetics of a small, artificially selected DNA aptamer with those of equivalently simple naturally occurring proteins. Protein Sci. 2014;23(1):56–66.
[54] Rosenberg JE, Bambury RM, Allen EMV. A phase II trial of AS1411 (a novel nucleolin-targeted DNA aptamer) in metastatic renal cell carcinoma. Invest New Drugs. 2014;32(1):178–187.
[55] Shu Y, Pi F, Sharma A. Stable RNA nanoparticles as potential new generation drugs for cancer therapy. Adv Drug Deliv Rev. 2014;66:74–89.
[56] Qiu M, Khisamutdinov E, Zhao Z. RNA nanotechnology for computer design and in vivo computation. Phil Trans R Soc A. 2013;371 (2000). 20120310.
[57] Rychahou P, Haque F, Shu Y. Delivery of RNA nanoparticles into colorectal cancer metastases following systemic administration. ACS Nano. 2015;9(2):1108–1116.
[58] Boero M. Leurs synthetase: a first-principles investigation of the water-mediated editing reaction. J Phys Chem B. 2011;115 (42):12276–12286.
[59] Hansson T, Oostenbrink C, van Gunsteren W. Molecular dynamics simulations. Curr Opin Struct Biol. 2002;12(2):190–196.
[60] Binder K, Horbach J, Kob W, et al. Molecular dynamics simulations. J Phys Condens Matter. 2004;16(5):S429.
[61] Andersen HC. Molecular dynamics simulations at constant pressure and/or temperature. J Chem Phys. 1980;72(4):2384–2393.
[62] Karplus M, McCammon JA. Molecular dynamics simulations of biomolecules. Nat Struct Mol Biol. 2002;9(9):646–652.
[63] Lindahl ER. Molecular dynamics simulations. Methods Mol Biol. 2008;443:3–23.
[64] Schlick T, Collepardo-Guevara R, Halvorsen LA, et al. Biomolecularmodeling and simulation: a field coming of age. Q Rev Biophys. 2011;44(2):191.
[65] Dror RO, Dirks RM, Grossman J, et al. Biomolecular simulation: a computational microscope for molecular biology. Annu Rev Biophys. 2012;41:429–452.
[66] Huggins DJ, Biggin PC, Dämgen MA, et al. Biomolecular simulations: from dynamics and mechanisms to computational assays of biological activity. Wiley Interdiscip Rev Comput Mol Sci. 2019;9(3):e1393.
[67] Verlet L. Computer 'experiments' on classical fluids. I. Thermodynamical properties of Lennard-Jones molecules. Phys Rev. 1967;159(1):98.
[68] Rapaport DC. The art of molecular dynamics simulation. Cambridge: Cambridge University Press; 2004.
[69] Sponer J, Bussi G, Krepl M, et al. RNA structural dynamics as captured by molecular simulations: a comprehensive overview. Chem Rev. 2018;118(8):4177–4338.
[70] Hashem Y, Auffinger P. A short guide for molecular dynamics simulations of RNA systems. Methods. 2009;47(3):187–197.
[71] Torsten S. Computational structural biology: methods and applications. Singapore: World Scientific; 2008.
[72] Dawson WK, Maciejczyk M, Jankowska EJ, et al. Coarse-grained modeling of RNA 3D structure. Methods. 2016;103:138–156.
[73] Singh N, Li W. Recent advances in coarse-grained models for biomolecules and their applications. Int J Mol Sci. 2019;20(15):3774.
[74] Noid WG. Perspective: coarse-grained models for biomolecular systems. J Chem Phys. 2013;139(9):09B201_1.
[75] Takada S. Coarse-grained molecular simulations of large biomolecules. Curr Opin Struct Biol. 2012;22(2):130–137.
[76] Riniker S, Allison JR, van Gunsteren WF. On developing coarse-grained models for biomolecular simulation: a review. Phys Chem Chem Phys. 2012;14(36):12423–12430.
[77] Ingólfsson HI, Lopez CA, Uusitalo JJ, et al. The power of coarse graining in biomolecular simulations. Wiley Interdisciplinary Rev: Comput Molecular Sci. 2014;4(3):225–248.
[78] Kmiecik S, Gront D, Kolinski M. Coarse-grained protein models and their applications. Chem Rev. 2016;116(14):7898–7936.
[79] Paliy M, Melnik R, Shapiro BA. Coarse-graining RNA nanostructures for molecular dynamics simulations. Phys Biol. 2010;7(3). 036001.
[80] Korolev N, Luo D, Lyubartsev AP, et al. A coarse-grained DNA model parameterized from atomistic simulations by inverse Monte Carlo. Polymers. 2014;6(6):1655–1675.
[81] Reith D, Pütz M, Müller-Plathe F. Deriving effective mesoscale potentials from atomistic simulations. J Comput Chem. 2003;24 (13):1624–1636.
[82] Lyubartsev AP, Laaksonen A. Calculation of effective interaction potentials from radial distribution functions: a reverse Monte Carlo approach. Phys Rev E. 1995;52(4):3730–3737.
[83] Ercolessi F, Adams JB. Interatomic potentials from first-principles calculations: the force-matching method. Euro Phys Lett. 1994;26 (8):583.
[84] Ouldridge TE, Louis AA, Doye JP. Structural, mechanical and thermodynamic properties of a coarse-grained DNA model. J Chem Phys. 2011;134(8):02B627.
[85] Korolev N, Nordenskiöld L, Lyubartsev AP. Multiscale coarse-grained modelling of chromatin components: DNA and the nucleosome. Adv Colloid Interface Sci. 2016;232:36–48.
[86] Mathieu F, Liao S, Kopatsch J. Six-helix bundles designed from DNA. Nano Lett. 2005;5(4):661–665.
[87] Bulacu M, Goga N, Zhao W, et al. Improved angle potentials for coarse-grained molecular dynamics simulations. J Chem Theory Comput. 2013;9(8):3282–3292.
[88] Bahar I, Rader A. Coarse-grained normal mode analysis in structural biology. Curr Opin Struct Biol. 2005;15(5):586–592.
[89] Tama F, Valle M, Frank J. Dynamic reorganization of the functionally active ribosome explored by normal mode analysis and cryo-electron microscopy. PNAS. 2003;100(16):9319–9323.
[90] Tozzini V. Coarse-grained models for proteins. Curr Opin Struct Biol. 2005;15(2):144–150.
[91] Hori N, Takada S. Coarse-grained structure-based model for RNA-protein complexes developed by fluctuation matching. J Chem Theory Comput. 2012;8(9):3384–3394.
[92] Das R, Baker D. Automated de novo prediction of native-like RNA tertiary structures. PNAS. 2007;104(37):14664–14669.
[93] Bernauer J, Huang X, Sim AYL. Fully differentiable coarse-grained and all-atom knowledge-based potentials for RNA structure evaluation. RNA. 2011;17(6):1066–1075.
[94] Ding F, Sharma S, Chalasani P. Ab initio RNA folding by discrete molecular dynamics: from structure prediction to folding mechanisms. RNA. 2008;14(6):1164–1173.
[95] Bida J, Das R. Squaring theory with practice in RNA design. Curr Opin Struct Biol. 2012;22(4):457–466.

[96] Xia Z, Gardner DP, Gutell RR. Coarse-grained model for simulation of RNA three-dimensional structures. J Phys Chem B. 2010;114(42):13497–13506.

[97] Draper DE, Grilley D, Soto AM. Ions and RNA folding. Annu Rev Biophys Biomol Struct. 2005;34(1):221–243.

[98] Woodson SA. Metal ions and RNA folding: a highly charged topic with a dynamic future. Curr Opin Chem Biol. 2005;9(2):104–109.

[99] Uusitalo JJ, Ingólfsson HI, Marrink SJ, et al. Martini coarse-grained force field: extension to RNA. Biophys J. 2017;113(2):246–256.

[100] Pasquali S, Derreumaux P. Hire-RNA: a high resolution coarse-grained energy model for RNA. J Phys Chem B. 2010;114(37):11957–11966.

[101] Cragnolini T, Derreumaux P, Pasquali S. Coarse-grained simulations of RNA and DNA duplexes. J Phys Chem B. 2013;117(27):8047–8060.

[102] Stadlbauer P, Mazzanti L, Cragnolini T, et al. Coarse-grained simulations complemented by atomistic molecular dynamics provide new insights into folding and unfolding of human telomeric G-quadruplexes. J Chem Theory Comput. 2016;12(12):6077–6097.

[103] Boniecki MJ, Lach G, Dawson WK, et al. Simrna: a coarse-grained method for RNA folding simulations and 3D structure prediction. Nucleic Acids Res. 2016;44(7):e63–e63.

[104] Šulc P, Romano F, Ouldridge TE, et al. A nucleotide-level coarse-grained model of RNA. J Chem Phys. 2014;140(23):06B614_1.

[105] Dans PD, Gallego D, Balaceanu A, et al. Modeling, simulations, and bioinformatics at the service of RNA structure. Chem. 2019;5(1):51–73.

[106] Zavadlav J, Arampatzis G, Koumoutsakos P. Bayesian selection for coarse-grained models of liquid water. Sci Rep. 2019;9(1):1–10.

[107] Schöberl M, Zabaras N, Koutsourelakis PS. Predictive collective variable discovery with deep Bayesian models. J Chem Phys. 2019;150(2):024109.

[108] Shi X, Wang X, Wang TL, et al. SparseIso: a novel Bayesian approach to identify alternatively spliced isoforms from RNA-seq data. Bioinformatics. 2018;34(1):56–63.

[109] Isralewitz B, Gao M, Schulten K. Steered molecular dynamics and mechanical functions of proteins. Curr Opin Struct Biol. 2001;11(2):224–230.

[110] Gullingsrud JR, Braun R, Schulten K. Reconstructing potentials of mean force through time series analysis of steered molecular dynamics simulations. J Comput Phys. 1999;151(1):190–211.

[111] Park S, Schulten K. Calculating potentials of mean force from steered molecular dynamics simulations. J Chem Phys. 2004;120(13):5946–5961.

[112] Patel JS, Berteotti A, Ronsisvalle S, et al. Steered molecular dynamics simulations for studying protein–ligand interaction in cyclin-dependent kinase 5. J Chem Inf Model. 2014;54(2):470–480.

[113] Uribe L, Gauss J, Diezemann G. Determining factors for the unfolding pathway of peptides, peptoids, and peptidic foldamers. J Phys Chem B. 2016;120(40):10433–10441.

[114] Mücksch C, Urbassek HM. Forced desorption of bovine serum albumin and lysozyme from graphite: insights from molecular dynamics simulation. J Phys Chem B. 2016;120(32):7889–7895.

[115] Mücksch C, Urbassek HM. Accelerating steered molecular dynamics: toward smaller velocities in forced unfolding simulations. J Chem Theory Comput. 2016;12(3):1380–1384.

[116] Mücksch C, Urbassek HM. Accelerated molecular dynamics study of the effects of surface hydrophilicity on protein adsorption. Langmuir. 2016;32(36):9156–9162.

[117] Paliy M, Melnik R, Shapiro BA. Molecular dynamics study of the RNA ring nanostructure: a phenomenon of self-stabilization. Phys Biol. 2009;6(4). 046003.

[118] Afonin KA, Kasprzak WK, Bindewald E. In silico design and enzymatic synthesis of functional RNA nanoparticles. Acc Chem Res. 2014;47(6):1731–1741.

[119] Parlea L, Bindewald E, Sharan R. Ring catalog: a resource for designing self-assembling RNA nanostructures. Methods. 2016;103:128–137.

[120] Kurkcuoglu O, Kurkcuoglu Z, Doruker P. Collective dynamics of the ribosomal tunnel revealed by elastic network modeling. Proteins. 2009;75(4):837–845.

[121] Deriu MA, Soncini M, Orsi M. Anisotropic elastic network modeling of entire microtubules. Biophys J. 2010 ;99(7):2190–2199.

[122] Ahmed A, Gohlke H. Multiscale modeling of macromolecular conformational changes combining concepts from rigidity and elastic network theory. Proteins. 2006;63(4):1038–1051.

[123] Khisamutdinov EF, Jasinski DL, Li H. Fabrication of RNA 3D nanoprisms for loading and protection of small RNAs and model drugs. Adv Mater. 2016;28(45):10079–10087.

[124] Westhof E, Masquida B, Jaeger L. RNA tectonics towards RNA design. Folding and Design. 1996;1(4):R78–R88.

[125] Yu J, Liu Z, Jiang W, et al. *De novo* design of an RNA tile that self-assembles into a homo-octameric nanoprism. Nat Commun. 2015;6(1):1–6.

[126] Severcan I, Geary C, Verzemnieks E. Square-shaped RNA particles from different RNA folds. Nano Lett. 2009;9(3):1270–1277.

[127] Boerneke MA, Dibrov SM, Hermann T. Crystal-structure-guided design of self-assembling RNA nanotriangles. Angew Chem Int Ed. 2016;55(12):4097–4100.

[128] Monferrer A, Zhang D, Lushnikov AJ, et al. Versatile kit of robust nanoshapes self-assembling from RNA and DNA modules. Nat Commun. 2019;10(1):1–8.

[129] Bell DR, Cheng SY, Salazar H, et al. Capturing RNA folding free energy with coarse-grained molecular dynamics simulations. Sci Rep. 2017;7(1):1–14.

[130] Li H, Wang S, Ji Z, et al. Construction of RNA nanotubes. Nano Res. 2019;12(8):1952–1958.

[131] Badu SR, Melnik R, Paliy MV, et al. High performance computing studies of RNA nanotubes. IWBBIO; 2014. p. 601–607.

[132] Badu S, Melnik R, Paliy M, et al. Modeling of RNA nanotubes using molecular dynamics simulation. Eur Biophys J. 2014;43(10–11):555–564.

[133] Belonenko M, Zhukov A, Paliy M, et al. The possibility of using RNA for optical applications. Bulletin of the Russian Academy of Sci: Phys. 2012;76(3):260–263.

[134] Lee AJ, Crothers DM. The solution structure of an RNA loop-loop complex: the ColE1 inverted loop sequence. Structure. 1998;6(8):993–1007.

[135] Tomizawa JI. Control of cole 1 plasmid replication: the process of binding of RNA I to the primer transcript. Cell. 1984;38(3):861–870.

[136] Tomizawa JI. Control of ColE1 plasmid replication: binding of RNA I to RNA II and inhibition of primer formation. Cell. 1986;47(1):89–97.

[137] Phillips JC, Braun R, Wang W, et al. Scalable molecular dynamics with NAMD. J Comput Chem. 2005;26(16):1781–1802.

[138] MacKerell Jr AD, Bashford D, Bellott M, et al. All-atom empirical potential for molecular modeling and dynamics studies of proteins. J Phys Chem B. 1998;102(18):3586–3616.

[139] Humphrey W, Dalke A, Schulten K. VMD: visual molecular dynamics. J Mol Graph. 1996;14(1):33–38.

[140] Feller SE, Zhang Y, Pastor RW. Constant pressure molecular dynamics simulation: the Langevin piston method. J Chem Phys. 1995;103(11):4613–4621.

[141] Martyna GJ, Tobias DJ, Klein ML. Constant pressure molecular dynamics algorithms. J Chem Phys. 1994;101(5):4177–4189.

[142] Badu SR, Melnik R, Prabhakar S. Transport properties of RNA nanotubes using molecular dynamics simulation. International Conference on Bioinformatics and Biomedical Engineering; Springer; 2015. p. 578–583.

[143] Badu S, Melnik R, Prabhakar S. Studying properties of RNA nanotubes via molecular dynamics. Nanosensors, Biosensors, and Info-Tech Sensors and Systems 2015; Vol. 9434, International Society for Optics and Photonics; 2015. p. 94340E.

[144] Badu S, Melnik R, Prabhakar S. RNA Nanostructures in physiological solutions: multiscale modeling and application. In: Physics of liquid matter: modern problems. Springer; 2015. p. 337–355.

[145] Badu S, Prabhakar S, Melnik R. Coarse-grained models of RNA nanotubes for large time scale studies in biomedical applications. Biomedicines. 2020;8(7):195.
[146] Naskar S, Joshi H, Chakraborty B, et al. Atomic structures of RNA nanotubes and their comparison with DNA nanotubes. Nanoscale. 2019;11(31):14863–14878.
[147] Leontis NB, SantaLucia J, Staff ACS. Molecular modeling of nucleic acids. Washington (DC): ACS Publications; 1998.
[148] Salomon-Ferrer R, Case DA, Walker RC. An overview of the Amber biomolecular simulation package. Wiley Interdiscip Rev Comput Molecular Sci. 2013;3(2):198–210.
[149] Kuzuya A, Wang R, Sha R, et al. Six-helix and eight-helix DNA nanotubes assembled from half-tubes. Nano Lett. 2007;7(6):1757–1763.
[150] Wang T, Schiffels D, Martinez Cuesta S, et al. Design and characterization of 1D nanotubes and 2D periodic arrays self-assembled from DNA multi-helix bundles. J Am Chem Soc. 2012;134(3):1606–1616.
[151] Endo M, Takeuchi Y, Emura T, et al. Preparation of chemically modified RNA origami nanostructures. Chem European J. 2014;20(47):15330–15333.
[152] Stewart JM, Geary C, Franco E. Design and characterization of RNA nanotubes. ACS Nano. 2019;13(5):5214–5221.
[153] Rafiee R, Moghadam RM. On the modeling of carbon nanotubes: a critical review. Compos B Eng. 2014;56:435–449.
[154] Cheng HC, Liu YL, Hsu YC, et al. Atomistic-continuum modeling for mechanical properties of single-walled carbon nanotubes. Int J Solids Struct. 2009;46(7-8):1695–1704.
[155] Wernik JM, Meguid SA. Atomistic-based continuum modeling of the nonlinear behavior of carbon nanotubes. Acta Mech. 2010;212(1-2):167–179.
[156] Li S, Urata S. An atomistic-to-continuum molecular dynamics: theory, algorithm, and applications. Comput Methods Appl Mech Eng. 2016;306:452–478.
[157] Ulz MH. Coupling the finite element method and molecular dynamics in the framework of the heterogeneous multiscale method for quasi-static isothermal problems. J Mech Phys Solids. 2015;74:1–18.
[158] Zhang L, Berlyand L, Fedorov MV, et al. Global energy matching method for atomistic-to-continuum modeling of self-assembling biopolymer aggregates. Multiscale Model Simul. 2010;8(5):1958–1980.
[159] Chen J, Garcia-Cervera CJ, Li X. An atomistic/continuum coupling method using enriched bases. Multiscale Model Simul. 2015;13(3):766–789.
[160] Luskin M, Ortner C. Atomistic-to-continuum coupling. Acta Numerica. 2013;22:397–508.
[161] Badu S, Prabhakar S, Melnik R, et al. Atomistic to continuum model for studying mechanical properties of RNA nanotubes. Comput Methods Biomech Biomed Eng. 2020;0:1–12.
[162] Badu S, Melnik R, Prabhakar S. Coupled nanostructures of ribonucleic acids: developing discrete-continuum models for large time-scale simulations. In: Coupled problems in science and engineering; 2017. p. 474–481.
[163] Badu S, Melnik R. Discrete-to-continuum models for biomedical applications of RNA nanotubes. 2017 IEEE 37th International Conference on Electronics and Nanotechnology (ELNANO); IEEE; 2017. p. 83–87.
[164] Badu S, Melnik R, Prabhakar S. RNA nanostructures in physiological solutions: multiscale modeling and applications. In: Physics of liquid matter: modern problems. Springer; 2015. p. 337–355.
[165] Chen JS, Lee CH, Teng H. Atomistic to continuum modeling of DNA molecules. In: Advances in soft matter mechanics. Springer; 2012. p. 1–53.
[166] Buehler MJ. Nanomechanics of collagen fibrils under varying cross-link densities: atomistic and continuum studies. J Mech Behav Biomed Mater. 2008;1(1):59–67.
[167] Depalle B, Qin Z, Shefelbine SJ, et al. Influence of cross-link structure, density and mechanical properties in the mesoscale deformation mechanisms of collagen fibrils. J Mech Behav Biomed Mater. 2015;52:1–13.
[168] Manning RS, Maddocks JH, Kahn JD. A continuum rod model of sequence-dependent DNA structure. J Chem Phys. 1996;105(13):5626–5646.
[169] Kim YJ, Kim DN. Structural basis for elastic mechanical properties of the DNA double helix. PLoS One. 2016;11(4):e0153228.
[170] Xiang P, Liew KM. Predicting buckling behavior of microtubules based on an atomistic-continuum model. Int J Solids Struct. 2011;48(11-12):1730–1737.
[171] Wurm P, Ulz MH. A stochastic approximation approach to improve the convergence behavior of hierarchical atomistic-to-continuum multiscale models. J Mech Phys Solids. 2016;95:480–500.
[172] Zajac M, Chakraborty K, Saha S, et al. What biologists want from their chloride reporters – a conversation between chemists and biologists. J Cell Sci. 2020;133(2):1.
[173] LaCasse Z, Briscoe JR, Nesterov EE, et al. Multidimensional tunability of nucleic acids enables sensing over unknown backgrounds. Anal Chem. 2019;91(22):14275–14280.
[174] Rong G, Tuttle EE, Neal Reilly A, et al. Recent developments in nanosensors for imaging applications in biological systems. Ann Rev Anal Chem. 2019;12:109–128.
[175] Sun Z, Nguyen T, McAuliffe K, et al. Intracellular imaging with genetically encoded RNA-based molecular sensors. Nanomaterials. 2019;9(2):233.
[176] Zheng XT, Lai YC, Tan YN. Nucleotide-derived theranostic nanodots with intrinsic fluorescence and singlet oxygen generation for bioimaging and photodynamic therapy. Nanoscale Adv. 2019;1(6):2250–2257.
[177] Samanta D, Ebrahimi SB, Mirkin CA. Nucleic-acid structures as intracellular probes for live cells. Advanced Mat. 2019.
[178] Chakraborty K, Veetil AT, Jaffrey SR, et al. Nucleic acid-based nanodevices in biological imaging. Ann Rev Biochem. 2016;85(1):349–373.
[179] Xie N, Huang J, Yang X. Competition-mediated FRET-switching DNA tetrahedron molecular beacon for intracellular molecular detection. ACS Sens. 2016;1(12):1445–1452.
[180] Sharma S, Visweswariah SS. Illuminating cyclic nucleotides: sensors for cAMP and cGMP and their application in live cell imaging. J Indian Inst Sci. 2017;97(1):109–128.
[181] Kumar P, Sharma PK, Nielsen P. Synthesis, hybridization and fluorescence properties of a 2$^\prime$-C-pyrene-triazole modified arabino-uridine nucleotide. Bioorg Med Chem. 2017;25(7):2084–2090.
[182] Li H, Shen W, Lam MHW, et al. Localized degradation of foreign DNA strands in cells: only excising the first nucleotide of 5′ region. Anal Biochem. 2017;533:10–17.
[183] You M, Jaffrey SR. Structure and mechanism of RNA mimics of green fluorescent protein. Annu Rev Biophys. 2015;44(1):187–206.
[184] Liu S, Jiang Q, Wang Y, et al. Biomedical applications of DNA-based molecular devices. Adv Healthc Mater. 2019;8(10):1801658.
[185] Chandrasekaran AR, Punnoose JA, Zhou L, et al. DNA nanotechnology approaches for microRNA detection and diagnosis. Nucleic Acids Res. 2019;47(20):10489–10505.
[186] Zhou YJ, Wan YH, Nie CP, et al. Molecular switching of a self-assembled 3D DNA nanomachine for spatiotemporal pH mapping in living cells. Anal Chem. 2019;91(16):10366–10370.
[187] Xue J, Chen F, Bai M, et al. All-in-one synchronized DNA nanodevices facilitating multiplexed cell imaging. Anal Chem. 2019;91(7):4696–4701.
[188] Shi H, Wang Y, Zheng J, et al. Dual-responsive DNA nanodevice for the available imaging of an apoptotic signaling pathway in situ. ACS Nano. 2019;13(11):12840–12850.
[189] Jiang Q, Zhao S, Liu J, et al. Rationally designed DNA-based nanocarriers. Adv Drug Deliv Rev. 2019;147:2–21.
[190] Dan K, Veetil AT, Chakraborty K, et al. DNA nanodevices map enzymatic activity in organelles. Nat Nanotechnol. 2019;14(3):252–259.

[191] Narayanaswamy N, Chakraborty K, Saminathan A, et al. A pH-correctable, DNA-based fluorescent reporter for organellar calcium. Nat Methods. 2019;16(1):95–102.
[192] Leung K, Chakraborty K, Saminathan A, et al. A DNA nanomachine chemically resolves lysosomes in live cells. Nat Nanotechnol. 2019;14(2):176–183.
[193] Zhang K, Yang XJ, Zhao W, et al. Regulation and imaging of gene expression via an RNA interference antagonistic biomimetic probe. Chemical Sci. 2017;8(7):4973–4977.
[194] Chen YJ, Groves B, Muscat RA. DNA nanotechnology from the test tube to the cell. Nat Nano. 2015;10(9):748–760.
[195] Surana S, Shenoy AR, Krishnan Y. Designing DNA nanodevices for compatibility with the immune system of higher organisms. Nat Nano. 2015;10(9):741–747.
[196] Serganov A. The long and the short of riboswitches. Curr Opin Struct Biol. 2009;19(3):251–259.
[197] Halman J, Satterwhite E, Smollett J. Triggerable RNA nanodevices. RNA & Disease. 2016;3(3):1.
[198] Afonin KA, Viard M, Tedbury P, et al. The use of minimal RNA toeholds to trigger the activation of multiple functionalities. Nano Lett. 2016 Mar;16(3):1746–1753.
[199] Zakrevsky P, Parlea L, Viard M. Preparation of a conditional RNA switch. In: RNA nanostructures. Springer; 2017. p. 303–324.
[200] Chandler M, Lyalina T, Halman J, et al. Broccoli fluorets: split aptamers as a user-friendly fluorescent toolkit for dynamic RNA nanotechnology. Molecules. 2018;23(12):3178.
[201] Endo K, Hayashi K, Saito H. Numerical operations in living cells by programmable RNA devices. Sci Adv. 2019;5(8):eaax0835.
[202] Zakrevsky P, Bindewald E, Humbertson H, et al. A suite of therapeutically-inspired nucleic acid logic systems for conditional generation of single-stranded and double-stranded oligonucleotides. Nanomaterials. 2019;9(4):615.
[203] Halman JR, Kim KT, Gwak SJ, et al. A cationic amphiphilic copolymer as a carrier of nucleic acid nanoparticles (Nanps) for controlled gene silencing, immunostimulation, and biodistribution. Nanomed Nanotechnol Biol Med. 2020;23:102094.
[204] Goldsworthy V, LaForce G, Abels S, et al. Fluorogenic RNA aptamers: a nano-platform for fabrication of simple and combinatorial logic gates. Nanomaterials. 2018;8(12):984.
[205] Di Lorenzo G, Ricci G, Severini GM, et al. Imaging and therapy of ovarian cancer: clinical application of nanoparticles and future perspectives. Theranostics. 2018;8(16):4279.
[206] Han X, Xu K, Taratula O, et al. Applications of nanoparticles in biomedical imaging. Nanoscale. 2019;11(3):799–819.
[207] Ruiz Ciancio D, Vargas MR, Thiel WH, et al. Aptamers as diagnostic tools in cancer. Pharmaceuticals. 2018;11(3):86.
[208] Wang Z, Wang J, Liu G. Theranostic magnetic nanoparticles as molecular imaging agents for siRNA delivery. In: Handbook of nanomaterials for cancer theranostics. Elsevier; 2018. p. 551–576.
[209] Bui MN, Brittany Johnson M, Viard M. Versatile RNA tetra-U helix linking motif as a toolkit for nucleic acid nanotechnology. Nanomed Nanotechnol Biol Med. 2017;13(3):1137–1146.
[210] Xu C, He XY, Peng Y, et al. A facile strategy to enhance specificity and sensitivity of molecular beacons by an aptamer functionalized delivery vector. Anal Chem. 2019.
[211] Zheng J, Yang R, Shi M, et al. Rationally designed molecular beacons for bioanalytical and biomedical applications. Chem Soc Rev. 2015;44(10):3036–3055.
[212] Han SX, Jia X, Ma Jl, et al. Molecular beacons: a novel optical diagnostic tool. Arch Immunol Ther Exp (Warsz). 2013;61(2):139–148.
[213] Lee T, Yagati AK, Pi F, et al. Construction of RNA–quantum dot chimera for nanoscale resistive biomemory application. ACS Nano. 2015;9(7):6675–6682.
[214] Xing X, Chen M, Gong Y, et al. Building memory devices from biocomposite electronic materials. Sci Technol Adv Mater. 2020;21(1):1.
[215] Jaeger L, Westhof E, Leontis NB. TectoRNA: modular assembly units for the construction of RNA nano-objects. Nucl Acids Res. 2001;29(2):455–463.
[216] Jaeger L, Chworos A. The architectonics of programmable RNA and DNA nanostructures. Curr Opin Struct Biol. 2006;16(4):531–543.
[217] Guo P. The emerging field of RNA nanotechnology. Nat Nano. 2010;5(12):833–842.
[218] Afonin KA, Lindsay B, Shapiro BA. Engineered RNA nanodesigns for applications in RNA nanotechnology. DNA and RNA Nanotechnology. 2013;1(1):1.
[219] Shukla GC, Haque F, Tor Y. A boost for the emerging field of RNA nanotechnology. ACS Nano. 2011;5(5):3405–3418.
[220] Afonin KA, Bindewald E, Yaghoubian AJ. In vitro assembly of cubic RNA-based scaffolds designed in silico. Nat Nano. 2010;5(9):676–682.
[221] Afonin KA, Grabow WW, Walker FM. Design and self-assembly of siRNA-functionalized RNA nanoparticles for use in automated nanomedicine. Nat Protocols. 2011;6(12):2022–2034.
[222] Afonin KA, Viard M, Koyfman AY. Multifunctional RNA nanoparticles. Nano Lett. 2014;14(10):5662–5671.
[223] Guo S, Huang F, Guo P. Construction of folate-conjugated pRNA of bacteriophage phi29 DNA packaging motor for delivery of chimeric siRNA to nasopharyngeal carcinoma cells. Gene Ther. 2006;13(10):814–820.
[224] Abdelmawla S, Guo S, Zhang L, et al. Pharmacological characterization of chemically synthesized monomeric phi29 pRNA nanoparticles for systemic delivery. Mol Ther. 2011;19(7):1312–1322.
[225] Shu D, Li H, Shu Y, et al. Systemic delivery of anti-miRNA for suppression of triple negative breast cancer utilizing RNA nanotechnology. ACS Nano. 2015;9(10):9731–9740.
[226] Cui D, Zhang C, Liu B, et al. Regression of gastric cancer by systemic injection of RNA nanoparticles carrying both ligand and siRNA. Sci Rep. 2015;5:10726.
[227] Ramezanpour M, Leung S, Delgado-Magnero K, et al. Computational and experimental approaches for investigating nanoparticle-based drug delivery systems. Biochimica Et Biophysica Acta (BBA)-Biomembranes. 2016;1858(7):1688–1709.
[228] Shamsi M, Mohammadi A, Manshadi MK, et al. Mathematical and computational modeling of nano-engineered drug delivery systems. J Control Release. 2019;307:150–165.
[229] Stojceski F, Grasso G, Pallante L, et al. Molecular and coarse-grained modeling to characterize and optimize dendrimer-based nanocarriers for short interfering RNA delivery. ACS Omega. 2020;5(6):2978–2986.
[230] Li J, Ouyang Y, Kong X, et al. A multi-scale molecular dynamics simulation of PMAL facilitated delivery of siRNA. RSC Adv. 2015;5(83):68227–68233.
[231] Verona MD, Verdolino V, Palazzesi F, et al. Focus on PNA flexibility and RNA binding using molecular dynamics and metadynamics. Sci Rep. 2017;7:42799.
[232] Rissanou A, Ouranidis A, Karatasos K. Complexation of single stranded rna with an ionizable lipid: an all-atom molecular dynamics simulation study. Soft Matter. 2020.
[233] Ohno H, Akamine S, Saito H. RNA nanostructures and scaffolds for biotechnology applications. Curr Opin Biotechnol. 2019;58:53–61.
[234] Pi F, Zhang H, Li H. RNA nanoparticles harboring annexin A2 aptamer can target ovarian cancer for tumor-specific doxorubicin delivery. Nanomed Nanotechnol Biol Med. 2017;13(3):1183–1193.
[235] Jang M, Han HD, Ahn HJ. A RNA nanotechnology platform for a simultaneous two-in-one siRNA delivery and its application in synergistic RNAi therapy. Sci Rep. 2016;6:32363.
[236] Pi F. RNA nanotechnology for next generation targeted drug delivery. Theses and Dissertations – Pharmacy, University of Kentucky; 2016. p. 65. Available from: https://doiorg/1013023/ETD2016432.
[237] Ishikawa J, Furuta H, Ikawa Y. RNA Tectonics (tectoRNA) for RNA nanostructure design and its application in synthetic biology. WIREs RNA. 2013;4(6):651–664.
[238] Suri SS, Fenniri H, Singh B. Nanotechnology-based drug delivery systems. J Occupational Med and Toxicology. 2007;2:16.

[239] Misra R, Acharya S, Sahoo SK. Cancer nanotechnology: application of nanotechnology in cancer therapy. Drug Discov Today. 2010;15 (19–20):842–850.
[240] Shi J, Votruba AR, Farokhzad OC. Nanotechnology in drug delivery and tissue engineering: from discovery to applications. Nano Lett. 2010;10(9):3223–3230.
[241] Patel MR, Kozuch SD, Cultrara CN. RNAi screening of the glucose-regulated chaperones in cancer with self-assembled siRNA nanostructures. Nano Lett. 2016;16(10):6099–6108.
[242] P Dabkowska A, Michanek A, Jaeger L, et al. Assembly of RNA nanostructures on supported lipid bilayers. Nanoscale. 2015;7 (2):583–596.
[243] Quader S, Kataoka K. Nanomaterial-enabled cancer therapy. Mol Ther. 2017;25(7):1501–1513.
[244] Burnett JC, Rossi JJ. RNA-based therapeutics: current progress and future prospects. Chem Biol. 2012;19(1):60–71.
[245] Thijssen MF, Brüggenwirth IM, Gillooly A, et al. Gene silencing with siRNA (RNA interference): a new therapeutic option during ex vivo machine liver perfusion preservation. Liver Transpl. 2019;25(1):140–151.
[246] Lee TJ, Haque F, Shu D, et al. RNA nanoparticle as a vector for targeted siRNA delivery into glioblastoma mouse model. Oncotarget. 2015;6(17):14766.
[247] Hill AC, Hall J. High-order structures from nucleic acids for biomedical applications. Materials Chemistry Frontiers. 2020;0:1.
[248] Wei X, Melnik RV, Moreno-Hagelsieb G. Modelling dynamics of genetic networks as a multiscale process. International Conference on Computational Science. Springer; 2005. p. 134–138.
[249] Reardon S. Step aside CRISPR, RNA editing is taking off. Nature. 2020;578(7793):24–27.
[250] Pei Y, Lu M. Programmable RNA manipulation in living cells. Cell Mol Life Sci. 2019;76:4861–4867.
[251] Kulkarni A, Yu W, Moon AS, et al. Programmable CRISPR interference for gene silencing using Cas13a in mosquitoes. bioRxiv. 2019;8:30.
[252] Kennedy EM, Bassit LC, Mueller H, et al. Suppression of hepatitis B virus DNA accumulation in chronically infected cells using a bacterial CRISPR/Cas RNA-guided DNA endonuclease. Virology. 2015;476:196–205.
[253] Ramanan V, Shlomai A, Cox DB, et al. CRISPR/Cas9 cleavage of viral DNA efficiently suppresses hepatitis B virus. Sci Rep. 2015;5:10833.
[254] Brüggenwirth IM, Martins PN. RNA interference therapeutics in organ transplantation: the dawn of a new era. Am J Transplant. 2019;20:931–941.
[255] Weissenbacher A, Vrakas G, Nasralla D, et al. The future of organ perfusion and re-conditioning. Transpl Int. 2019;32(6):586–597.
[256] Buchwald JE, Xu J, Bozorgzadeh A, et al. Therapeutics administered during ex vivo liver machine perfusion: an overview. World J Transplant. 2020;10(1):1.
[257] Demirer GS, Zhang H, Goh NS, et al. Carbon nanocarriers deliver siRNA to intact plant cells for efficient gene knockdown. bioRxiv. 2019;6:564427.
[258] Zakrevsky P, Kasprzak WK, Heinz WF, et al. Truncated tetrahedral RNA nanostructures exhibit enhanced features for delivery of RNAi substrates. Nanoscale. 2020;12:1.
[259] Yingchoncharoen P, Kalinowski DS, Richardson DR. Lipid-based drug delivery systems in cancer therapy: what is available and what is yet to come. Pharmacol Rev. 2016;68(3):701–787.
[260] Duncan R. Polymer therapeutics as nanomedicines: new perspectives. Curr Opin Biotechnol. 2011;22(4):492–501.
[261] Lee KL, Twyman RM, Fiering S, et al. Virus-based nanoparticles as platform technologies for modern vaccines. Wiley Interdiscip Rev Nanomed Nanobiotechnology. 2016;8(4):554–578.
[262] Sun W, Mignani S, Shen M, et al. Dendrimer-based magnetic iron oxide nanoparticles: their synthesis and biomedical applications. Drug Discov Today. 2016;21(12):1873–1885.
[263] van der Meel R, Vehmeijer LJ, Kok RJ, et al. Ligand-targeted particulate nanomedicines undergoing clinical evaluation: current status. Adv Drug Deliv Rev. 2013;65(10):1284–1298.
[264] Lammers T, Kiessling F, Hennink WE, et al. Drug targeting to tumors: principles, pitfalls and (pre-) clinical progress. J Control Release. 2012;161(2):175–187.
[265] Binzel DW, Shu Y, Li H, et al. Specific delivery of miRNA for high efficient inhibition of prostate cancer by RNA nanotechnology. Mol Ther. 2016;24(7):1267–1277.
[266] Shu Y, Haque F, Shu D, et al. Fabrication of 14 different RNA nanoparticles for specific tumor targeting without accumulation in normal organs. RNA. 2013;19(6):767–777.
[267] Rychahou P, Haque F, Shu Y, et al. Delivery of RNA nanoparticles into colorectal cancer metastases following systemic administration. ACS Nano. 2015;9(2):1108–1116.
[268] Zhou J, Shu Y, Guo P, et al. Dual functional RNA nanoparticles containing phi29 motor pRNA and anti-gp120 aptamer for cell-type specific delivery and HIV-1 inhibition. Methods. 2011;54 (2):284–294.
[269] Feng L, Li SK, Liu H, et al. Ocular delivery of pRNA nanoparticles: distribution and clearance after subconjunctival injection. Pharm Res. 2014;31(4):1046–1058.
[270] Guo S, Xu C, Yin H, et al. Tuning the size, shape and structure of RNA nanoparticles for favorable cancer targeting and immunostimulation. Wiley Interdiscip Rev Nanomed Nanobiotechnology. 2020;12(1):e1582.
[271] Shin H, Park SJ, Yim Y, et al. Recent advances in RNA therapeutics and RNA delivery systems based on nanoparticles. Adv Therapeutics. 2018;1(7):1800065.
[272] Tekade RK, Tekade M, Kesharwani P. RNAi-combined nano-chemotherapeutics to tackle resistant tumors. Drug Discov Today. 2016;21(11):1761–1774.
[273] Mi Y, Shao Z, Vang J. Application of nanotechnology to cancer radiotherapy. Cancer Nano. 2016;7(1):11.
[274] Zhang C, Zhou Z, Zhi X, et al. Insights into the distinguishing stress-induced cytotoxicity of chiral gold nanoclusters and the relationship with GSTP1. Theranostics. 2015;5(2):134.
[275] Borghei YS, Hosseini M, Ganjali MR. Label-free fluorescent detection of microRNA-155 based on synthesis of hairpin DNA-templated copper nanoclusters by etching (top-down approach). Sensors and Actuators B: Chemical. 2017;248:133–139.
[276] Bergs JWJ, Wacker MG, Hehlgans S. The role of recent nanotechnology in enhancing the efficacy of radiation therapy. Biochimica Et Biophysica Acta (BBA) – Reviews on Cancer. 2015;1856(1):130–143.
[277] Gomes-da Silva LC, Simões S, Moreira JN. Challenging the future of siRNA therapeutics against cancer: the crucial role of nanotechnology. Cell Mol Life Sci. 2014;71(8):1417–1438.
[278] Jasinski DL, Yin H, Li Z, et al. Hydrophobic effect from conjugated chemicals or drugs on in vivo biodistribution of RNA nanoparticles. Hum Gene Ther. 2018;29(1):77–86.
[279] Lee JH, Ku SH, Kim MJ, et al. Rolling circle transcription-based polymeric siRNA nanoparticles for tumor-targeted delivery. J Control Release. 2017;263:29–38.
[280] Guo Y, Li S, Wang Y, et al. Diagnosis–therapy integrative systems based on magnetic RNA nanoflowers for co-drug delivery and targeted therapy. Anal Chem. 2017;89(4):2267–2274.
[281] Zhang Y, Leonard M, Shu Y, et al. Overcoming tamoxifen resistance of human breast cancer by targeted gene silencing using multifunctional pRNA nanoparticles. ACS Nano. 2017;11(1):335–346.
[282] Souza AG, Marangoni K, Fujimura PT. 3D Cell-SELEX: development of RNA aptamers as molecular probes for PC-3 tumor cell line. Exp Cell Res. 2016;341(2):147–156.
[283] Liu R, Mu LM, Bai J, et al. Development of double strand RNA mPEI nanoparticles and application in treating invasive breast cancer. RSC Adv. 2019;9(23):13186–13200.
[284] Bakshi S, Zakharchenko A, Minko S, et al. Towards nanomaterials for cancer theranostics: a system of DNA-modified magnetic nanoparticles for detection and suppression of RNA marker in cancer cells. Magnetochemistry. 2019;5(2):24.
[285] Yin H, Xiong G, Guo S, et al. Delivery of anti-miRNA for triple-negative breast cancer therapy using RNA nanoparticles targeting stem cell marker CD133. Mol Ther. 2019;27(7):1252–1261.

[286] Nam J, Son S, Park KS, et al. Cancer nanomedicine for combination cancer immunotherapy. Nature Rev Mat. 2019;4(6):398–414.
[287] Takefuji Y, Ben-Alon D, Zaritsky A. Neural computing in discovering RNA interactions. Biosystems. 1992;27(2):85–96.
[288] Zhang H, Zhang C, Li Z, et al. A new method of RNA secondary structure prediction based on convolutional neural network and dynamic programming. Front Genet. 2019;10:1.
[289] Singh J, Hanson J, Paliwal K, et al. RNA secondary structure prediction using an ensemble of two-dimensional deep neural networks and transfer learning. Nat Commun. 2019;10(1):1–13.
[290] Wolfe BR, Porubsky NJ, Zadeh JN, et al. Constrained multistate sequence design for nucleic acid reaction pathway engineering. J Am Chem Soc. 2017;139(8):3134–3144.
[291] Anderson-Lee J, Fisker E, Kosaraju V, et al. Principles for predicting RNA secondary structure design difficulty. J Mol Biol. 2016;428(5):748–757.
[292] Kerpedjiev P, Hammer S, Hofacker IL. Forna (force-directed RNA): simple and effective online RNA secondary structure diagrams. Bioinformatics. 2015;31(20):3377–3379.
[293] Kerpedjiev P, Zu Siederdissen CH, Hofacker IL. Predicting RNA 3D structure using a coarse-grain helix-centered model. RNA. 2015;21(6):1110–1121.
[294] Lee J, Kladwang W, Lee M, et al. RNA design rules from a massive open laboratory. Proc National Academy of Sci. 2014;111(6):2122–2127.
[295] Zhao Y, Huang Y, Gong Z, et al. Automated and fast building of three-dimensional RNA structures. Sci Rep. 2012;2:734.
[296] Reinharz V, Major F, Waldispühl J. Towards 3D structure prediction of large RNA molecules: an integer programming framework to insert local 3D motifs in RNA secondary structure. Bioinformatics. 2012;28(12):i207–i214.
[297] Taneda A. MODENA: a multi-objective RNA inverse folding. Adv Appl Bioinform Chem. 2011;4:1.
[298] Busch A, Backofen R. INFO-RNA-a server for fast inverse RNA folding satisfying sequence constraints. Nucleic Acids Res. 2007;35(2):W310–W313.
[299] Andronescu M, Fejes AP, Hutter F, et al. A new algorithm for RNA secondary structure design. J Mol Biol. 2004;336(3):607–624.
[300] Hofacker IL. Vienna RNA secondary structure server. Nucleic Acids Res. 2003;31(13):3429–3431.
[301] Deng D, Holman D, Hendrix DA. DeepSloop: a recurrent neural network learns complex rules to detect stem-loop-forming RNA sequences. 2019 IEEE International Conference on Bioinformatics and Biomedicine (BIBM); IEEE; 2019. p. 2799–2807.
[302] Nussinov R, Pieczenik G, Griggs JR, et al. Algorithms for loop matchings. SIAM J Appl Math. 1978;35(1):68–82.
[303] Zuker M, Stiegler P. Optimal computer folding of large RNA sequences using thermodynamics and auxiliary information. Nucleic Acids Res. 1981;9(1):133–148.
[304] Zuker M. Mfold web server for nucleic acid folding and hybridization prediction. Nucleic Acids Res. 2003;31(13):3406–3415.
[305] Zou Q, GUO Mz, ZHANG Tt. A review of RNA secondary structure prediction algorithms. Acta Electronica Sinica. 2008;36(2):331.
[306] Hofacker IL, Fontana W, Stadler PF, et al. Fast folding and comparison of RNA secondary structures. Monatshefte Für Chemie/Chemical Monthly. 1994;125(2):167–188.
[307] Knudsen B, Hein J. Using stochastic context free grammars and molecular evolution to predict RNA secondary structure. Bioinformatics. 1999;15(6):446–454.
[308] Sankoff D. Simultaneous solution of the RNA folding, alignment and protosequence problems. SIAM J Appl Math. 1985;45(5):810–825.
[309] Allali J, Sagot MF. A new distance for high level RNA secondary structure comparison. IEEE/ACM Trans Comput Biol Bioinform. 2005;2(1):3–14.
[310] Hu YJ. GPRM: a genetic programming approach to finding common RNA secondary structure elements. Nucleic Acids Res. 2003;31(13):3446–3449.
[311] Zhang X, Deng Z, Song D. Neural network approach to predict RNA secondary structures. J Tsinghua Univ (Sci Technol). 2006;10:1.
[312] Steeg EW. Neural networks, adaptive optimization, and RNA secondary structure prediction. Artif Intell Mol Biol. 1993;0:121–160.
[313] Liu W, Wang Z, Liu X, et al. A survey of deep neural network architectures and their applications. Neurocomputing. 2017;234:11–26.
[314] Wang S, Peng J, Ma J, et al. Protein secondary structure prediction using deep convolutional neural fields. Sci Rep. 2016;6(1):1–11.
[315] Koodli RV, Keep B, Coppess KR, et al. EternaBrain: Automated RNA design through move sets and strategies from an Internet-scale RNA videogame. PLoS Comput Biol. 2019;15(6):e1007059.
[316] Chen X, Li Y, Umarov R, et al. RNA secondary structure prediction by learning unrolled algorithms; 2020. p. 1. arXiv preprint arXiv:200205810.
[317] Runge F, Stoll D, Falkner S, et al. Learning to design RNA; 2018. p. 1. arXiv preprint arXiv:181211951.